
Value-Based Abstraction Functions for Abstraction Sampling

Bobak Pezeshki¹

Kalev Kask¹

Alexander Ihler¹

Rina Dechter¹

¹University of California, Irvine

Abstract

Monte Carlo methods are powerful tools for solving problems involving complex probability distributions. Despite their versatility, these methods often suffer from inefficiencies, especially when dealing with rare events. As such, importance sampling emerged as a prominent technique for alleviating these challenges. Recently, a new scheme called Abstraction Sampling was developed that incorporated stratification to importance sampling over graphical models. However, existing work only explored a limited set of abstraction functions that guide stratification. This study introduces three new classes of abstraction functions combined with seven distinct partitioning schemes, resulting in twenty-one new abstraction functions, each motivated by theory and intuition from both search and sampling domains. An extensive empirical analysis on over 400 problems compares these new schemes highlighting several well-performing candidates.

1 INTRODUCTION

The partition function (Z) is an important quantity in probabilistic graphical model inference and is often estimated using Monte Carlo methods such as Importance Sampling (IS) [Rubinstein and Kroese, 2016, Liu et al., 2015, Gogate and Dechter, 2011]. Inspired by the works of Knuth [1975] and Chen [1992], a framework called Abstraction Sampling (AS) [Broka et al., 2018] was introduced extending IS by enabling samples to represent multiple configurations. AS uses concepts from Stratified Sampling [Rubinstein and Kroese, 2016, Rizzo, 2007] and Compact Search [Dechter and Mateescu, 2007, Marinescu and Dechter, 2009] to build a sampled subtree called a *probe* which is then used to compute an estimate. Probes are built level-by-level according to a variable ordering where, at each level, an *abstraction function* groups nodes into *abstract states* from which representative nodes are selected to extend paths in the probe.

Using what are referred to as context-based abstraction functions, Broka et al. [2018] showed competitive performance of AS against IS, Weighted Mini-Bucket Importance Sampling (wMBIS) [Liu et al., 2015, Ihler et al., 2012], and IJGP-SampleSearch (IJGP-ss) [Gogate and Dechter, 2011]. Kask et al. [2020] improved Abstraction Sampling scalability with the AOAS algorithm that more efficiently applied AS to AND/OR search spaces. AOAS showed improved performance, additionally comparing to state-of-the-art scheme Dynamic Importance Sampling (DIS) [Lou et al., 2019].

However, AS development has lacked exploration of diverse and potentially more effective abstraction functions. While Hsiao et al. [2023] proposed using graph neural networks to learn abstraction functions, such methods require learning on a corpus of similar problems before use.

Contributions. This work provides a detailed study of new abstraction schemes for AS. We present a new class of abstractions defined by real-valued functions aimed at capturing relevant similarity features between nodes. Three classes of this new framework are introduced and augmented by seven partitioning strategies. A purely randomized scheme is also introduced. An extensive empirical evaluation is performed on over 400 problems, comparing our novel schemes against: each other, the previous relCB and randCB abstraction functions [Broka et al., 2018, Kask et al., 2020], and implicitly against IS, wMBIS, IJGP-ss, and DIS.

Our experiments identify three schemes in particular that perform significantly better than any previous scheme. Our results demonstrate a significant improvement for one of the most competitive sampling schemes, thus also yielding a substantial computational advance for one of the most challenging tasks in probabilistic inference.

2 GENERAL BACKGROUND

Graphical Models. A *graphical model*, such as a Bayesian or Markov network [Pearl, 1988, Darwiche, 2009, Dechter, 2013], can be defined by a 3-tuple $\mathcal{M} = (\mathbf{X}, \mathbf{D}, \mathbf{F})$,

where \mathbf{X} is a set of variables, and \mathbf{D} is the set of variable domains, and \mathbf{F} is a set of functions such that each function $f_\alpha \in \mathbf{F}$ is defined over a subset of variables $\alpha \subseteq \mathbf{X}$ (called the function’s scope) capturing local interactions. \mathcal{M} defines a global function, often a factorized probability distribution on \mathbf{X} , $P(\mathbf{X}) = \frac{1}{Z} \prod_\alpha f_\alpha(X_\alpha)$, where $Z = \sum_{\mathbf{X}} \prod_\alpha f_\alpha(X_\alpha)$, known as the partition function, is a normalization factor. A *primal graph* $\mathcal{G} = (\mathbf{V}, \mathbf{E})$ of \mathcal{M} associates each variable with a node ($\mathbf{V} = \mathbf{X}$) with edges $e \in \mathbf{E}$ connecting nodes whose variables interact locally, appearing in the scope of the same functions.

Search Spaces of Graphical Models. A graphical model can be transformed into a compact AND/OR search space to leverage conditional independence and facilitate efficient search algorithms [Dechter and Mateescu, 2007].

Given a primal graph \mathcal{G} , an AND/OR search space is defined relative to a *pseudo tree* $\mathcal{T} = (\mathbf{V}, \mathbf{E}')$, a directed rooted tree that captures conditional independence encoded in the model. A pseudo tree \mathcal{T} is constructed according to a variable ordering such that every arc of \mathcal{G} not in \mathbf{E}' is a back-arc in \mathcal{T} . This construction ensures conditional independence of any variable and its descendants from variables found in the other branches of \mathcal{T} given assignments to their common ancestors. The pseudo tree in Figure 1a was constructed using a variable ordering $o = [A, B, C, D]$. The dashed line shows an edge in the primal graph that is missing from \mathcal{T} , but that would be a back-arc if it were present. From its structure we see that variables C and D are independent of B given assignment to A . Here A is referred to as a *branching variable* since it branches to multiple children.

Guided by a pseudo tree \mathcal{T} , an *AND/OR search tree* T has alternating levels of OR nodes corresponding to variables and AND nodes corresponding to possible assignments to those variables. Figure 1 shows an AND/OR search tree and its guiding pseudo tree. Note that in the pseudo tree, variables B and C extend to different branches from A . Similarly, in the AND/OR search tree, we see OR nodes B and C extending to different branches under each possible assignment of A . An arc into an AND node n_X of variable X has a cost $c(n_X)$ equal to the product of functions $f_\alpha \in \mathbf{F}$ such that the path to n_X fully instantiates all $X' \in \alpha$ and such that $X \in \alpha$ [Dechter and Mateescu, 2007].

Notation. Capital letters (X) represent variables and small letters (x) their values. Boldfaced letters represent a collection. Boldfaced capital letters (\mathbf{X}) denote a collection of variables, $|\mathbf{X}|$ its cardinality, $D_{\mathbf{X}}$ their joint domains (all possible configurations of \mathbf{X}), and bolded x a particular realization in that joint domain (a particular configuration of \mathbf{X}).

In the context of search, n is used generally to represent nodes in a search tree. For AND/OR search trees, n_X is used to specifically refer to an AND node associated with variable X , and Y_{n_X} the OR node associated with variable

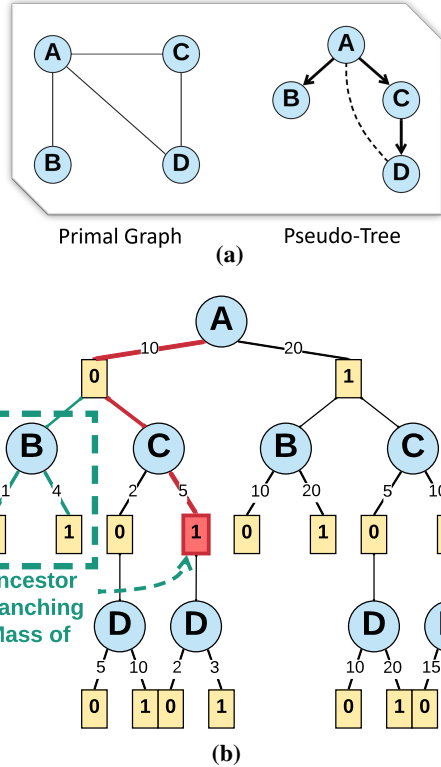


Figure 1: A full AND/OR tree representing 16 possible full configurations of binary variables A, B, C , and D guided by the pseudo tree shown in subfigure (a) above. The path cost for the highlighted node $n_{A=0,C=1}$ at the end of the path $\rightarrow(A=0) \rightarrow(C=1)$ is $g(n_{A=0,C=1}) = 10 \cdot 5$. The value of the subtree under $n_{A=0,C=1}$ is $Z(n_{A=0,C=1}) = 2 \cdot 1 + 3 \cdot 1$. Boxed in green is the ancestor branching subtree for $n_{A=0,C=1}$ and it has the value $R(n_{A=0,C=1}) = 1 \cdot 1 + 4 \cdot 1$. Thus, $Q(n_{A=0,C=1}) = (10 \cdot 5) \cdot (1 \cdot 1 + 4 \cdot 1) \cdot (2 \cdot 1 + 3 \cdot 1)$.

Y that is the child of n_X . $ch(n)$ are the children of node n . $path(n)$ is the configuration of the variables along the path from the root of a search tree T to node n according to assignments corresponding to that path. For the highlighted node n in Figure 1b, $path(n) = \{A=0, C=1\}$. $varpath(n)$ is the set of variables that $path(n)$ provides a configuration for. In Figure 1b $varpath(n) = \{A, C\}$. The cost of the arc to an AND node n_X is

$$c(n_X) = \prod_{f \in \{f_\alpha \in \mathbf{F} \mid \alpha \subseteq varpath(n_X), X \in \alpha\}} f(path(n_X)). \quad (1)$$

or 1, vacuously. Letting $anc(n)$ be the AND node ancestors of n in the search tree, the cost of $path(n)$ is $g(n) = \prod_{n' \in anc(n)} c(n')$. In Figure 1b, $g(n) = 10 \cdot 5$.

We now define some important quantities involved in evaluating AND/OR search spaces.

$Z(n)$. The total cost of the subtree rooted at n . For an AND node n_X with children OR nodes $Y_{n_X} \in ch(n_X)$, $Z(n_X)$ satisfies

$$Z(n_X) = \prod_{Y_{n_X} \in ch(n_X)} Z(Y_{n_X}) \quad (2)$$

such that for OR nodes Y_{n_X}

$$Z(Y_{n_X}) = \sum_{n_Y \in ch(Y_{n_X})} c(n_Y) \cdot Z(n_Y) \quad (3)$$

with $Z(n_X) = 1$ in the case n_X has no children.

Note that given n_\emptyset as the dummy root node of AND/OR tree T , $Z(n_\emptyset) = Z$ of the underlying model \mathcal{M} . We denote estimation of $Z(n)$ as $\hat{Z}(n)$. Heuristic estimates of $Z(n)$ are more specifically denoted as $h(n)$.

R(n). On the path from the root of an AND/OR tree T to some node n_X , there may be an intermediate node n_Y associated with branching variable Y in the guiding pseudo tree \mathcal{T} . (In Figure 1b, on the path to the highlighted node $n_{A=0,C=1}$, node $n_{A=0}$ is traversed where A is a branching variable in \mathcal{T} of Figure 1a). When this happens, the remaining variables of the model are split between different branches. Thus, the $Z(n)$ of any node down one of the branches will necessarily omit the costs from the configurations of the variables included in the other branch(es). $R(n_X)$, or the *ancestor branching mass*, captures these omitted costs. (In Figure 1b, the green box shows the portion of T corresponding to $R(n_{A=0,C=1})$).

More formally, let $br(n_X)$ be the set of ancestor nodes n_{Y_i} of n_X such that each Y_i is a branching variable ancestor of X in \mathcal{T} . We then define $R(n_X)$ simply as:

$$R(n_X) = \prod_{n_Y \in br(n_X)} \prod_{\substack{W_{n_Y} \in ch(n_Y) \\ W_{n_Y} \notin path(n_X)}} Z(W_{n_Y}), \quad (4)$$

(In Figure 1b, $br(n_{A=0,C=1}) = \{n_{A=0}\}$, A being the only branching variable ancestor of C in \mathcal{T} , and $B_{n_{A=0}}$ the only respective child OR node **not** on the path to $n_{A=0,C=1}$. Thus, $R(n_{A=0,C=1}) = Z(B_{n_{A=0}})$). We denote approximations to $R(n)$ as $r(n)$.

Q(n). We can now concisely define a quantity $Q(n)$ as the contribution to Z from all full configurations consistent with $path(n)$. In other words, $Q(n)$ is the unnormalized measure of the configuration $path(n)$, with $P(path(n)) = \frac{Q(n)}{Z}$. The quantity $Q(n)$ obeys:

$$Q(n) = g(n) \cdot R(n) \cdot Z(n). \quad (5)$$

Example. In Figure 1b, consider the path from the root to the red node $n_{A=0,C=1}$. Following $n_{A=0}$ to our node, we see OR node $B_{n_{A=0}}$ branches off of the path. So,

$$\begin{aligned} Q(n_{A=0,C=1}) &= g(n_{A=0,C=1}) \cdot R(n_{A=0,C=1}) \cdot Z(n_{A=0,C=1}) \\ &= g(n_{A=0,C=1}) \cdot Z(B_{n_{A=0}}) \cdot Z(n_{A=0,C=1}) \\ &= (10 \cdot 5) \cdot (1 \cdot 1 + 4 \cdot 1) \cdot (2 \cdot 1 + 3 \cdot 1) \end{aligned}$$

Stratified Importance Sampling. Abstraction Sampling builds on Stratified Importance Sampling, which in turn builds on Importance Sampling and Stratified Sampling. *Importance Sampling* is a Monte Carlo scheme used for approximating likelihood queries [Rubinstein and Kroese, 2016, Liu et al., 2015, Gogate and Dechter, 2011]. *Stratified*

Algorithm 1: AOAS Overview

1. **Initialization:** Begin with a dummy root node r .
 2. **Probe Generation:** Proceeding in a DFS manner according to a pseudo tree \mathcal{T} ...
 - (a) **Expansion:** Generate children nodes n corresponding to the next variable in the DFS ordering of \mathcal{T} . Inherit $w(n)$ from parents and assign appropriate $g(n), h(n)$, and $r(n)$ values.
 - (b) **Abstraction:**
 - i. **Form Abstract States:** Using $a(\cdot)$, partition newly expanded nodes into abstract states.
 - ii. **Select Representative:** Using proposal $p(n) \propto q(n)$, stochastically select a representative from each abstract state and reweigh it such that $w(n) \leftarrow \frac{w(n)}{p(n)}$
 - (c) **Backtrack:** After reaching a leaf in \mathcal{T} , recursively backtrack until reaching the node that extends to the next unexplored branch of \mathcal{T} . While backtracking, update parent node n' 's $\hat{Z}(n')$ estimates based on its children's $w(n), g(n)$, and $\hat{Z}(n)$ values.
 - (d) **Repeat:** Repeat steps 2a-2c until backtracking to the root node.
 3. **Return:** $\hat{Z} = w(r) \hat{Z}(r)$ for the root node r .
-

Sampling is a variance reduction technique for sampling a search space by first dividing it into disjoint strata [Rubinstein and Kroese, 2016]. In *Stratified Importance Sampling*, the sample space is first divided into k strata, then representatives from each strata chosen and re-weighted to represent the omitted members of their respective strata. Rizzo [2007] shows that to reduce overall variance given strata of equal mass under the proposal, the sum of the variances within the strata should be minimized.

3 ABSTRACTION SAMPLING

Abstraction Sampling (AS) [Broka et al., 2018] applies concepts of Stratified Importance Sampling to sampling over probabilistic graphical models. AS is guided by an abstraction function $a(\cdot)$ that dictates how nodes are partitioned into *abstract states* (abstract states being analogous to strata in stratified sampling). A search tree is iteratively expanded along a variable ordering. After each expansion, $a(\cdot)$ is used to group nodes into abstract states. Then AS uses an importance-sampling-like process to select a representative from each abstract state and reweights it using importance sampling weights to account for the unselected nodes it represents. The selected nodes are then further expanded and the process iterates. This process yields a weighted sampled subtree of the full search tree T as a sample, referred to as a *probe*. It is important to note that AS probes can contain multiple full configurations, whereas samples from importance sampling are each only a single full configuration.

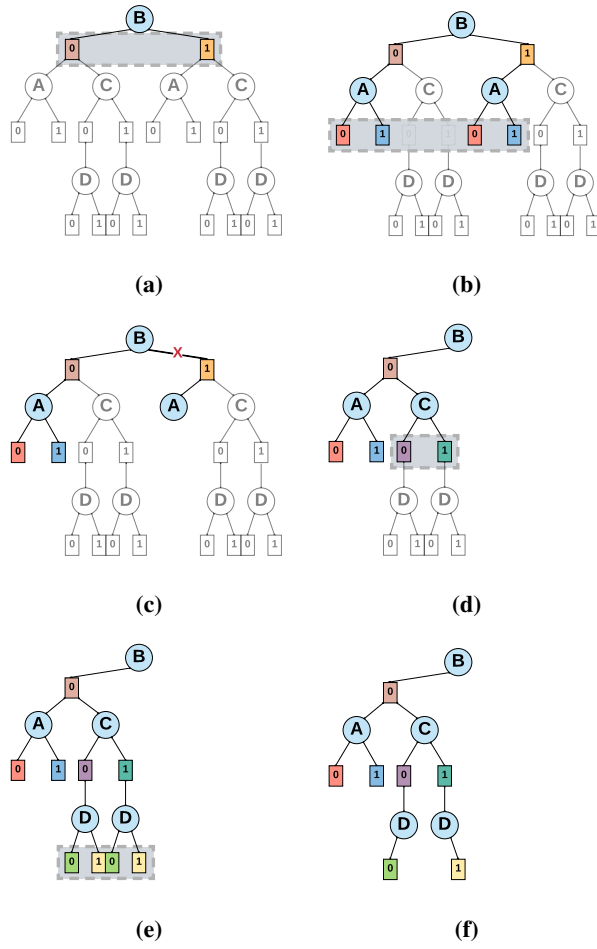


Figure 2: From Kask et al. [2020], a sample trace of AOAS following ordering $B \rightarrow A \rightarrow C \rightarrow D$. Transparent nodes indicate portions of the reachable search space yet to be explored. Gray boxes indicate nodes considered for abstraction. Nodes with the same domain values (also indicated by the same color) are abstracted into the same abstract state. Only one node of each color is stochastically selected as a representative for its respective abstract state. Step (c) shows an optional pruning step. Step (f) shows the final probe capturing four full configurations: $B=0, A=0, C=0, D=0$, $B=0, A=1, C=0, D=0$, $B=0, A=0, C=1, D=1$, $B=1, A=1, C=1, D=1$.

AOAS. Taking Abstraction Sampling further, Kask et al. [2020] introduced algorithm AOAS that more effectively applied Abstraction Sampling to AND/OR search spaces and significantly improved its performance. AOAS uses a proposal function $p(n) \propto w(n)q(n) = w(n)g(n)h(n)r(n)$ where a weight $w(n)$ accounts for the nodes previously abstracted into the path to n , $g(n)$ is the cost of the path to n , $h(n)$ is a heuristic estimate of $Z(n)$, and $r(n)$ is an estimate of $R(n)$ (see Figure 3). Algorithm 1 provides a high level description of the AOAS procedure. Figure 2 shows a sample trace of AOAS from Kask et al. [2020]. A more detailed version of the algorithm and detailed description of the sample trace can be found in the Supplemental Materials.

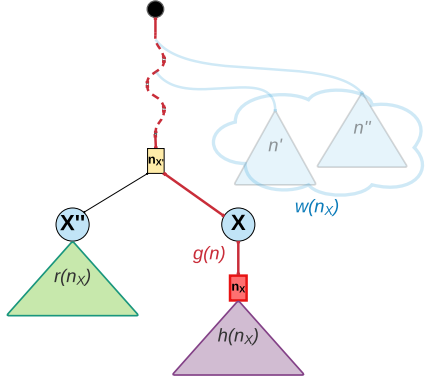


Figure 3: The unnormalized proposal distribution $w(n)q(n)$ visualized to show it considering nodes previously abstracted (via $w(n)$), the ancestor branching mass (via $r(n)$), current path cost (via $g(n)$), and subtree mass (via $h(n)$).

4 VALUE-BASED ABSTRACTIONS

The choice of abstraction function is a crucial aspect of Abstraction Sampling but has only received limited attention so far. The main focus of this work is to identify new abstraction functions that significantly improve AS performance.

Existing State-of-the-Art: Context-Based Abstraction Functions. Broka et al. [2018] designed abstractions based on assignments to a variable’s context $C(X)$ - a subset of its ancestors in \mathcal{T} whose assignments uniquely determine the AND/OR subtree below it [Dechter and Mateescu, 2007]. However, the number of configurations to a context is exponential in the context’s size. Thus, Broka et al. [2018] and Kask et al. [2020] used *relaxed* context-based (*RelCB*) and *randomized* context-based (*RandCB*) abstractions to control the number of abstract states. RelCB uses a parameter n_{Ctx} that groups nodes with the same configuration over the most recent $n_{Ctx} - 1$ context variables (the relaxed context) into the same abstract state. With a domain size of k , this yields at most $k^{n_{Ctx}}$ abstract states at each level. RandCB considers the entire context but bounds the number of abstract states per level based on an n_{Abs} parameter and by using a randomized hashing scheme to associate each full context assignment to one of the n_{Abs} abstract states.

Value-Based Abstractions. We now introduce a new way to form abstractions that we call Value-Based Abstractions. They are defined by (1) a positive real-valued function $\mu : D_X \rightarrow \mathbb{R}^+$, where D_X is a set of configurations for the variables X , and by (2) a partitioning scheme ψ_μ that assigns nodes to abstract states based on their μ value and in an order-consistent manner as defined next.

Definition 4.1 (Value-Ordered Partitioning)

Given n_{Abs} and a function $\mu : D_X \rightarrow \mathbb{R}^+$, a partitioning function $\psi_\mu : D_X \rightarrow \{A_1, A_2, \dots, A_{n_{Abs}}\}$, is order-consistent with μ relative to the n_{Abs} abstract states if for any $n_1 \in A_i$ and $n_2 \in A_j$, $i < j \Leftrightarrow \mu(n_1) \leq \mu(n_2)$.

4.1 VALUE-BASED ABSTRACTION CLASSES

We introduce three Value-Based Abstraction classes, each characterized by a unique value function μ that signifies a notion of similarity between nodes. We will subsequently provide partitioning schemes that, together with μ , will yield a set of full abstraction functions.

1. Heuristic-Based Abstractions. Heuristic-Based (HB) abstractions use $\mu(n) = h(n)$, where $h(n)$ is a heuristic estimate of $Z(n)$. Unlike partial or hashed contexts as used by Broka et al. [2018], heuristic estimates of $Z(n)$ can often provide quantitative insight into potential similarities of $Z(n)$ values. In particular, this intuition holds when using heuristics that provide bounds on $Z(n)$ such as those via Weighted Mini-Bucket Elimination (wMBE) [Dechter and Rish, 2003, Liu and Ihler, 2011].

2. Heuristic and Ancestral Branching-Based Abstractions. Recall that $r(n)$ is an estimate of n 's ancestor branching mass $R(n)$. We can show that:

Theorem 4.1 (AOAS Exact Abstractions)

If an abstraction function $a(\cdot)$ forms abstract states $A_i \in \mathcal{A}$ such that $\exists c_i \in \mathbb{R}^+, \forall n \in A_i, \frac{h(n)r(n)}{Z(n)R(n)} = c_i$ whenever $Z(n)R(n) > 0$ (or $h(n)r(n) = 0$ otherwise), then AOAS is exact with its estimates having zero variance.

This observation suggests to use $\text{ht}(n) = \frac{h(n)r(n)}{Z(n)R(n)}$ as a similarity measure. When nodes having close ht values are placed in the same abstract state it can lead to a reduction in variance of the resulting estimate. However, without access to $Z(n)$ or $R(n)$ we cannot evaluate this ratio directly. Instead we use the intuition that grouping based on $h(n)r(n)$ may result in sets of nodes also with similar $Z(n)R(n)$, and thus result in similar $\text{ht}(n)$. We call such schemes that use $\mu(n) = h(n)r(n)$ HR-Based (HRB) abstractions.

3. Q-Based Abstractions. Another intuition for generating abstractions comes from statistics theory. In his work on stratified Importance Sampling, Rizzo [2007] showed the potential of overall variance reduction by forming strata (abstract states) having equal mass under the proposal distribution and that minimizes the variance within each strata. Thus, since our proposal p is proportional to $w(n)q(n)$, we use $\mu(n) = w(n)q(n) = w(n)g(n)h(n)r(n)$ in what are called Q-based (QB) abstractions.

4.2 ORDERED PARTITIONING SCHEMES

Next we describe seven partitioning schemes ψ to be used with μ to partition the nodes \mathbf{n} into abstract states. Together, μ and ψ define a value-based abstraction function.

Running Example. We will use a running example to illustrate the result of using various partitioning schemes.

Assume we have eight nodes with the following $\mu(n)$:

$$1.0, 1.1, 1.2, 1.3, 1.4, 1.5, 10, 100 \quad (6)$$

Algorithm 2: $\Psi_{simpleVB}$

```

1  $baseCardinality \leftarrow \lfloor \frac{|\mathbf{n}|}{nAbs} \rfloor$ 
2  $extras \leftarrow |\mathbf{n}| \bmod nAbs$ 
3  $\mathbf{n}^* \leftarrow SORT(\mathbf{n}, \mu, \text{low-to-high})$ 
4  $jbegin \leftarrow 1$ 
5 foreach  $i \leftarrow 1, \dots, nAbs$  do
6   if  $extras > 0$  then
7      $jend \leftarrow jbegin + baseCardinality$ 
8      $extras \leftarrow extras - 1$ 
9   else
10     $jend \leftarrow jbegin + baseCardinality - 1$ 
11     $A_i \leftarrow \{n_{jbegin}^*, \dots, n_{jend}^*\}$ 
12     $jbegin \leftarrow jend + 1$ 
13 end
14  $A \leftarrow \cup_{i=1}^{nAbs} A_i$ 
15 return  $A$ 

```

and want to partition the nodes into $nAbs = 4$ abstract states. As we describe each partitioning scheme, we also demonstrate how the scheme would partition these nodes.

1. SimpleVB. The *simpleVB* (simple value-based) scheme groups nodes having similar $\mu(n)$ into the same state by a simple 2-step process: 1) nodes are ordered by $\mu(n)$ (low to high), and 2) nodes are partitioned into abstract states with [approximately] equal cardinality.

Running Example: {1.0, 1.1}, {1.2, 1.3}, {1.4, 1.5}, {10, 100}.

This method leverages speed while still aiming to roughly group nodes with similar $\mu(n)$ together.

2. minVarVB. *minVarVB* uses Ward's Minimum Variance Hierarchical Clustering, also known as Ward's Method [Ward, 1963] (Algorithm 3), to cluster nodes into $nAbs$ abstract states. Use of Ward's method minimizes total within variance of $\mu(\cdot)$ across all abstract states. Ward's Method can be combined with Lance-Williams linear distance updates [Lance and Williams, 1967] to increase efficiency. More details on Ward's Method and Lance-Williams linear distance updates are found in the Supplemental Materials.

Running Example: {1.0, 1.1, 1.2}, {1.3, 1.4, 1.5}, {10}, {100}.

In contrast to *simpleVB*, *minVarVB* places considerable computational resources into computing abstractions by using Ward's Method. Thus *minVarVB* leads to fewer probes being generated but provably forms abstractions that minimize the total within variance of $\mu(n)$ among the abstract states.

3. equalDistVB. In attempt to combine the intuition from *minVarVB* and the speed of *simpleVB*, *equalDistVB* greedily adds nodes in order of μ (low to high) into an abstract state A_i until

$$\mu(A_1, \dots, i) = \sum_{j=1}^i \sum_{n \in A_j} \mu(n) \geq \mathcal{Q}_i = \frac{i \cdot \sum_{n' \in \mathbf{n}} \mu(n')}{nAbs}, \quad (7)$$

i.e., until the total sum of node values from A_1, \dots, A_i reaches or exceeds $\frac{i}{nAbs}$ of the total across all of the nodes

Algorithm 3: Ward's Method

1. **Initialization:** Treat each data point as an individual cluster. Assign each cluster a label.
 2. **Compute Pairwise Distances:** Calculate the pairwise distances between all clusters. Various distance metrics can be used, such as Euclidean distance.
 3. **Cluster Merging Iteration:**
 - (a) Identify the pair of clusters C_i and C_j that, when merged into a new cluster C_{ij} , results in the smallest increase in the overall within-cluster variance. This is determined using the formula:

$$\Delta Var = Var(C_{ij}) - (Var(C_i) + Var(C_j))$$

where $Var(C_{ij})$ is the variance of the merged cluster, and $Var(C_i)$ and $Var(C_j)$ are the variances of clusters C_i and C_j , respectively.
 - (b) Update distance measures between the newly merged cluster and all other clusters.
 4. **Repeat:** Repeat steps 2-3 until the desired number of clusters is achieved.
-

being partitioned. When paired with Q-based abstractions, *equalDistVB* aims to partition nodes into equal mass states under the proposal, motivated by Rizzo [2007].

Running Example: {1.0, 1.1, 1.2, 1.3, 1.4, 1.5, 10, 100}, {}, {}, {}, {}.

Although *equalDistVB* hopes to strike a balance between efficiency and low variance of $\mu(n)$ within each abstract state, from the running example we can see it may yield undesirable partitionings for skewed distributions of $\mu(\cdot)$ values. In the example, all of the nodes need to be placed into the first of four abstract states before the sum of their values reaches/exceeds $\frac{1}{4}$ of the total of all nodes being partitioned. Thus, the remaining abstract states end up empty.

4. equalDistVB2. A second version of the *equalDist* scheme, *equalDistVB2*, follows the same general strategy as *equalDistVB* but uses a reversed sort ordering in attempt to mitigate overfilling of abstract states. Modifying the sort order from **low-to-high** to **high-to-low** in Line 1 of Algorithm 4 converts *equalDistVB* to *equalDistVB2*.

Running Example: {100}, {}, {}, {10, 1.5, 1.4, 1.3, 1.2, 1.1, 1.0}

We see that *equalDistVB2* can still over-pack abstract states. The next two variants aim to mitigate this issue further.

5. equalDistVB3. In order to further lessen over-packing and ensure abstract states are not left empty, *equalDistVB3* modifies *equalDistVB2* so that, after processing each abstract state, the next state always has a node added to it by default before checking the abstract state fill condition. Modifying the sort order from **low-to-high** to **high-to-low** in Line 1 and $A_i \leftarrow \{\}$ to $A_i \leftarrow \{n_j^*\}; j \leftarrow j + 1$; in Line 4 of Algorithm 4 converts *equalDistVB* to *equalDistVB3*.

Running Example: {100}, {10}, {1.5}, {1.4, 1.3, 1.2, 1.1, 1.0}.

Algorithm 4: $\Psi_{equalDistVB}$

- 1 $n^* \leftarrow SORT(n, \mu, \text{low-to-high})$
 - 2 $j \leftarrow 1$
 - 3 **foreach** $i \leftarrow 1, \dots, nAbs$ **do**
 - 4 $A_i \leftarrow \{\}$
 - 5 **while** $\mu(A_1, \dots, i) < Q_i$ **do**
 - 6 $A_i \leftarrow A_i \cup \{n_j^*\}$
 - 7 $j \leftarrow j + 1$
 - 8 **end**
 - 9 **end**
 - 10 $A \leftarrow \cup_{i=1}^{nAbs} A_i$
 - 11 **return** A
-

While still very efficient, *equalDistVB3* ensures that the provided $nAbs$ granularity is honored, allowing users better control of the search vs. sampling interpolation possible with Abstraction Sampling.

6. equalDistVB4. The final *equalDist* variant, *equalDistVB4*, aims for more even partitioning. Before processing each abstract state A_i , a new cut-off is determined based the remaining nodes n_{rm}^* and remaining abstract states:

$$\hat{Q}_i = \frac{\sum_{n \in n_{rm}^*} \mu(n)}{nAbs - i + 1}. \quad (8)$$

Nodes are added to abstract state A_i while $\mu(A_i) < \hat{Q}_i$. Modifying the sort order from **low-to-high** to **high-to-low** in Line 1 and $\mu(A_1, \dots, i) < Q_i$ to $\mu(A_i) < \hat{Q}_i$ in Line 5 of Algorithm 4 converts *equalDistVB* to *equalDistVB4*.

Running Example: {100}, {10}, {1.5, 1.4, 1.3}, {1.2, 1.1, 1.0}.

Still computationally efficient, *equalDistVB4* spreads nodes with small values more evenly across abstract states.

7. randVB. It can be beneficial to rely on randomness to ensure a diverse sampling of abstractions. *randVB* does this by sampling $nAbs - 1$ partition points uniformly at random and without replacement from between nodes sorted according to $\mu(\cdot)$, and then partitions the nodes accordingly. The resulting abstract states ensure that nodes are still grouped according to $\mu(\cdot)$, but the sizes of those groups vary.

Algorithm 5: Ψ_{randVB}

- 1 $s \sim Unif(\{M \subseteq \{1, \dots, |n| - 1\} \mid |M| = nAbs - 1\})$
 - 2 $s^* \leftarrow SORT(s)$
 - 3 $n^* \leftarrow SORT(n, \mu, \text{high-to-low})$
 - 4 $j \leftarrow 1$
 - 5 **foreach** $i \leftarrow 1, \dots, nAbs - 1$ **do**
 - 6 $A_i \leftarrow \{n_j^*, \dots, n_{s_i^*}^*\}$
 - 7 $j \leftarrow s_i^* + 1$
 - 8 **end**
 - 9 $A_{nAbs} = \{n_j^*, \dots, n_{|n^*|}^*\}$
 - 10 $A \leftarrow \cup_{i=1}^{nAbs} A_i$
 - 11 **return** A
-

Running Example: ex1: {100, 10}, {1.5}, {1.4, 1.3, 1.2}, {1.1, 1.0}; ex2: {100}, {10, 1.5, 1.4, 1.3}, {1.2, 1.1}, {1.0}; etc.

Complexity. Assuming $\mu(\cdot)$ is $\mathcal{O}(1)$, each of the proposed partitioning schemes have time complexity $\mathcal{O}(|n| \log |n|)$ and space complexity $\mathcal{O}(|n|)$, with the exception of *minVarVB*, which requires $\mathcal{O}(|n|^2)$ for both. More details can be found in the Supplemental Materials.

5 RANDOM-ONLY ABSTRACTIONS

Another unexplored approach was to use purely randomized abstraction schemes. At first glance, one may not expect such schemes to perform well, but randomization in concert with an informative heuristic and proposal can be beneficial.

Intuition. First, given an informative heuristic, the stochastic selection of a representative node *within* each abstract state using a good proposal function will typically opt for nodes that represent greater mass, which is generally beneficial in importance sampling. Second, the randomness of node assignments to the abstract states enables nodes that may otherwise have little chance of being selected to occasionally have a greater chance of selection, leading to a more diverse distribution of probes.

The simpleRand Scheme. More concisely referred to as **RAND**, the simpleRand scheme partitions nodes via a 2-step process: 1) nodes first are shuffled to create a uniformly random permutation, and then 2) the nodes are partitioned into (approximately) equal cardinality $nAbs$ abstract states.

Algorithm 6: $\Psi_{simpleRand}$

```

1  $baseCardinality \leftarrow \lfloor \frac{|n|}{nAbs} \rfloor$ 
2  $extras \leftarrow |n| \bmod nAbs$ 
3  $n^* \leftarrow RANDOM\_SHUFFLE(n)$ 
4  $jbegin \leftarrow 1$ 
5 foreach  $i \leftarrow 1, \dots, nAbs$  do
6   if  $extras > 0$  then
7      $jend \leftarrow jbegin + baseCardinality$ 
8      $extras \leftarrow extras - 1$ 
9   else
10     $jend \leftarrow jbegin + baseCardinality - 1$ 
11     $A_i \leftarrow \{n_{jbegin}^*, \dots, n_{jend}^*\}$ 
12     $jbegin \leftarrow jend + 1$ 
13 end
14  $A \leftarrow \cup_{i=1}^{nAbs} A_i$ 
15 return  $A$ 

```

Running Example: $\{1.4, 1.1\}, \{1.2, 10\}, \{1.0, 1.3\}, \{100, 1.5\}$.

Complexity. Both time and space are $\mathcal{O}(|n|)$.

6 EMPIRICAL EVALUATION

Overview. All combinations of Value-Based Abstraction Classes: Heuristic-Based (**HB**), HR-Based (**HRB**), and Q-Based (**QB**); with each of the Ordered Partitioning Schemes: *simpleVB*, *minVarVB*, *equalDistVB1-4*, and *randVB*; were

tested, resulting in twenty-one value-based abstraction functions. The formerly evaluated context-based (**CTX**) abstraction functions: randCB and relCB were compared against. In addition, the purely random abstraction function, **RAND**, was also included. With the exception of RelCB, each abstraction function uses a hyper parameter, $nAbs$, which bounds the number of abstract states at any level. RelCB instead uses an $nCtx$ parameter that limits the number of context variables used in assigning abstract states. To facilitate comparison, we report RelCB’s $nCtx$ parameter instead as an equivalent $nAbs$ parameter assuming a domain size of 2. (For example, if RelCB was run using $nCtx = 6$, we report it with $nAbs = 2^6$). All abstraction functions were tested using the AOAS algorithm [Kask et al., 2020]. All algorithms were implemented in C++. All experiments were run on a 2.66 GHz processor and allotted 8 GB of memory.

Heuristics. To inform the sampling proposal, Weighted Mini-Bucket Elimination (wMBE) [Dechter and Rish, 2003, Liu and Ihler, 2011] – which pairs well with AND/OR search [Mateescu and Dechter, 2005] – is used as a heuristic. The i-bound (**iB**) parameter controls the strength of wMBE, where higher i-bounds generally lead to stronger heuristics, and thus better proposals, at the expense of more computation and memory. We standardize our experiments by using the same i-bound when comparing across algorithms.

Benchmarks. In line with previous work on Abstraction Sampling, we perform experiments on the same set of over 400 problems from five benchmarks: DBN, Grids, Linkage-Type4, Pedigree, and Promedas used by Kask et al. [2020]. We refer to problem instances with known Z values as *Exact*. Larger problems without exact solutions are called *LARGE*. For LARGE problems, estimates from 10hr of AOAS using the RAND - RAND being well performing - are used as the reference Z value. When experimenting

Table 1: Exact Benchmark Statistics. Average statistics for Exact problems. N: number of instances, $|X|$: average number of variables, k: average of problems’ largest domain sizes, w^* : average induced tree-width, d: average \mathcal{T} depth.

Benchmark	N	$ X $	k	w^*	d
DBN	66	67	2	29	30
Grids	8	250	2	22	49
Pedigree	25	690	5	25	89
Promedas	65	612	2	21	62

Table 2: LARGE Benchmark Statistics. Average statistics for LARGE problems. N: number of instances, $|X|$: average number of variables, k: average of problems’ largest domain sizes, w^* : average induced tree-width, d: average \mathcal{T} depth.

Benchmark	N	$ X $	k	w^*	d
DBN	48	216	2	78	78
Grids	19	3432	2	117	220
Linkage-Type4	82	6550	5	45	761
Promedas	173	1194	2	72	114

on Exact problems, algorithms use a small i-bound of 5 (weakening the heuristic estimates) and were given a limited time of 300sec to increase difficulty. For LARGE problems, an i-bound of 10 and time limit of 1200sec are used.

Performance Measure. To evaluate performance, we define error as: $Error = |\log_{10} \hat{Z} - \log_{10} Z^*|$, where \hat{Z} is the estimate obtained from AS and Z^* is the reference Z value. For Exact problems, $Z^* = Z$.

6.1 RESULTS

Summary Comparison. To examine potential of the different methods, we tested each algorithm with a range of $nAbs \in \{1, 4, 16, 64, 256, 512, 1024, 2048\}$. For each $nAbs$ and benchmark, we calculated the average error across problems of the benchmark and identified the $nAbs$ that resulted in the lowest average error. Table 3a focuses on Exact problems and shows this lowest average error and corresponding $nAbs$ for each algorithm. Table 3b shows the corresponding results for LARGE problems on the better performing QB and RAND classes, and the CTX class for comparison. If an algorithm was unable to produce a positive Monte Carlo Z estimate for a problem (denoted "Fail"), the wMBE heuristic bound was used as its Z estimate and error computed accordingly. We highlight the best performing schemes.

Comparison using 100 Samples. To assess the quality of abstraction functions in an implementation-agnostic manner and irrespective of resulting probe-sizes or speed, we conducted experiments using a one-hundred sample limit (**m-100**). Table 4 shows these results on Exact problems for the better performing QB and Rand classes using $nAbs = 256$. $nAbs = 256$ was chosen as (1) it is an intermediate granularity and (2) all schemes produced 100 samples in a reasonable time. We highlight the best performing schemes.

Varying nAbs. Table 5 shows average error for $nAbs \in \{4, 64, 1024\}$ on Exact problems of each benchmark. We focus on the better performing variants of QB: minVarQB, equalDistQB3, equalDistQB4; the purely randomized scheme RAND; and the context-based schemes (CTX) for comparison. In Figure 4 and Figure 5, we also show average error across a wider array of $nAbs$ for minVarQB and equalDistQB4, respectively, the latter also acting as a representative for the profile of equalDistQB3 and RAND.

Time Series Plot. Figure 6 and Figure 7 show time-series results for the better performing QB algorithms, RAND, and CTX schemes on a representative Grids and Promedas problem. Each algorithm was plotted with the $nAbs$ that resulted in the lowest average error for the respective benchmark.

6.2 ANALYSIS

Comparison with Context-Based Schemes. Table 3a shows that there is always a partitioning scheme for HB and HRB that can outperform the best CTX scheme on Exact

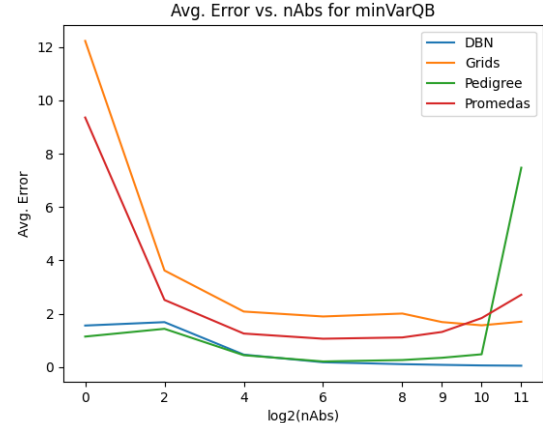


Figure 4: Varying $nAbs$ for minVarQB. Average error on Exact problems using iB-5 and time limit 300 sec for each benchmark at various abstraction granularities (in \log_2).

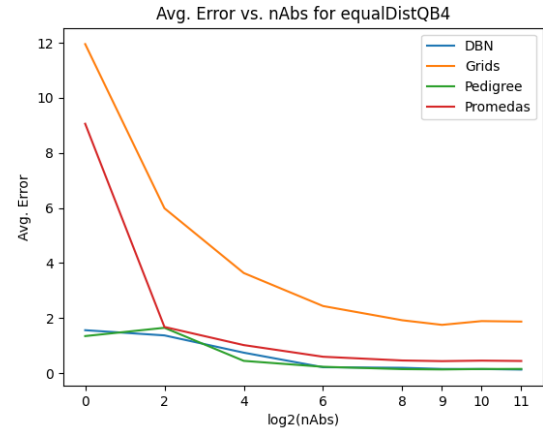


Figure 5: Varying $nAbs$ for equalDistQB4. Average error on Exact problems using iB-5 and time limit 300 sec for each benchmark at various abstraction granularities (in \log_2).

problems. For HB, the *simple* and *rand* partitioning schemes perform best, whereas for the HRB class it is more benchmark dependent. QB with *minVar*, *equalDist3*, and *equalDist4* partitioning outperform the CTX schemes across all benchmarks. RAND also consistently outperforms the CTX schemes. Results from Table 3b on LARGE problems agree, with the exception of QB with *minVar* and RAND, which fall slightly shy of randCB's performance on Promedas.

Comparison with Purely Randomized Abstractions. Table 3 shows RAND is a particularly well performing scheme across all benchmarks. However, the QB class using the *equalDist3* and *equalDist4* strategies is consistently comparable or better than the purely randomized scheme. No other scheme does as well.

Comparison with Non Abstraction Sampling Schemes. In prior work by Broka et al. [2018] and Kask et al. [2020], Abstraction Sampling using CTX based abstractions was shown as competitive against several powerful schemes such as Importance Sampling (IS), Weighted Mini-Bucket Importance Sampling (wMBIS) [Liu et al., 2015], IJGP-

iB-5, t-300sec, Exact		DBN			Grids			Pedigree			Promedas		
Class	Scheme	nAbs	Fail	Avg. Error	nAbs	Fail	Avg. Error	nAbs	Fail	Avg. Error	nAbs	Fail	Avg. Error
HB	simple	2048	0	0.440	1024	0	2.202	2048	0	0.150	1024	0	0.575
	minVar	1	0	1.361	16	0	3.251	64	0	0.422	16	2	2.509
	equalDist	1	0	1.365	2048	0	10.854	1024	0	0.303	1024	0	2.332
	equalDist2	1	0	1.570	512	0	8.050	1024	0	0.315	64	0	2.123
	equalDist3	1	0	1.489	2048	0	2.764	1024	0	0.279	256	0	2.196
	equalDist4	1024	0	2.819	64	0	6.029	512	0	0.214	2048	0	1.355
HRB	rand	256	0	0.496	2048	0	2.248	2048	0	0.185	2048	0	0.752
	simple	2048	0	0.491	4	0	9.667	256	0	0.225	2048	0	0.705
	minVar	1	0	1.500	64	0	2.319	256	0	0.309	16	1	2.801
	equalDist	1	0	1.305	256	0	10.635	1024	0	0.638	16	4	4.055
	equalDist2	1	0	1.549	2048	0	6.790	16	0	0.457	16	2	3.445
	equalDist3	1	0	1.405	1024	0	2.292	16	0	0.537	16	2	2.656
QB	equalDist4	1	0	1.511	512	0	1.829	64	0	0.483	2048	0	2.024
	rand	2048	0	0.451	4	0	6.122	64	0	0.666	1024	1	2.165
	simple	1	0	1.469	16	0	10.076	256	0	0.297	256	1	3.164
	minVar	2048	0	0.050	1024	0	1.566	64	0	0.210	64	1	1.062
	equalDist	4	0	1.174	2048	0	8.134	2048	0	0.144	2048	0	0.583
	equalDist2	2048	0	0.736	2048	0	4.405	1024	0	0.145	2048	0	0.539
CTX	equalDist3	2048	0	0.042	2048	0	1.771	512	0	0.148	2048	0	0.412
	equalDist4	2048	0	0.130	512	0	1.754	512	0	0.134	512	0	0.437
	rand	1	0	1.295	256	0	6.048	16	0	0.740	16	2	5.988
	rand	4	0	1.381	4	0	5.030	16	0	0.540	1024	1	2.442
	rel	1	0	1.472	64	0	4.021	64	0	0.424	64	6	4.349
RAND	rand	2048	0	0.104	1024	0	1.501	1024	0	0.143	1024	0	0.513

(a)

iB-10, t-1200sec, LARGE		DBN			Grids			Linkage-Type4			Promedas		
Class	Scheme	nAbs	Fail	Avg. Error	nAbs	Fail	Avg. Error	nAbs	Fail	Avg. Error	nAbs	Fail	Avg. Error
QB	simple	1	0	6.540	16	0	197.931	2048	13	48.681	4	34	11.919
	minVar	2048	0	1.837	1024	0	28.423	256	31	93.058	16	13	5.403
	equalDist	512	0	5.423	2048	0	118.547	2048	22	46.196	512	15	5.960
	equalDist2	2048	0	3.813	2048	0	91.994	1024	21	40.310	2048	12	4.982
	equalDist3	2048	0	1.645	2048	0	19.277	1024	20	37.490	256	5	2.560
	equalDist4	2048	0	1.643	2048	0	18.866	2048	16	30.512	512	5	2.476
CTX	rand	4	0	6.292	16	0	163.973	256	17	156.992	4	28	11.532
	rand	64	0	5.710	512	0	111.104	2048	53	194.741	256	0	3.222
	rel	1	0	6.267	1024	0	80.633	1024	37	129.189	16	34	11.247
	rand	2048	0	2.123	2048	0	19.053	1024	19	33.804	1024	10	3.936
RAND	rand	2048	0	2.123	2048	0	19.053	1024	19	33.804	1024	10	3.936

(b)

Table 3: Summary Comparison. Each table shows the Abstraction Class (*Class*), Partitioning Scheme (*Scheme*), bound on the number of abstract states per level (*nAbs*), number of problems for which a positive solution could not be estimated (*Fail*), and average $\log_{10} Z$ error (Avg. Error) across Exact problems (subtable (a)) and LARGE problems (subtable (b)) in each benchmark. Color bars visualize error magnitudes. We highlight the best performing algorithms: those for which: (1) difference in total average error (summed across the benchmarks) with respect to the best such total was less than 15% of the best, and (2) within each individual benchmark, the difference in average error with respect to the best average error was less than 35% of the best. (An exception to the latter criterion was granted to Exact DBN, on which the best average error from equalDistQB3 was unusually low).

iB-5, m-100, Exact		DBN			Grids			Pedigree			Promedas		
Class	Scheme	nAbs	Fail	Avg. Error	Fail	Avg. Error	Fail	Avg. Error	Fail	Avg. Error	Fail	Avg. Error	Fail
QB	simpleQB	256	0	5.350	0	17.406	0	1.059	14	9.659	4	34	11.919
	minVarQB	256	0	0.111	0	1.911	0	0.223	1	1.634	64	0	1.062
	equalDist	256	0	5.619	0	15.533	1	0.858	13	5.420	1024	0	0.403
	equalDist2	256	0	2.319	0	11.220	0	0.563	6	3.479	2048	0	0.210
	equalDist3	256	0	0.173	0	3.615	0	0.206	1	1.473	64	0	0.479
	equalDist4	256	0	0.277	0	2.305	0	0.180	1	1.373	1024	0	0.483
CTX	randQB	256	0	4.982	0	12.653	0	3.211	13	19.441	4	1.371	0
	rand	256	0	3.587	0	9.568	2	4.695	3	14.386	64	0	0.215
	rel	256	0	5.265	0	8.013	0	1.097	36	10.845	1024	0	0.150
	rand	256	0	0.288	0	2.464	0	0.325	3	2.570	2048	0	0.455
RAND	rand	2048	0	0.288	0	2.464	0	0.325	3	2.570	1024	0	0.513

Table 4: 100-Sample Comparison. For abstraction granularity of *nAbs* = 256, aggregated statistics (as described in Table 3) for Exact problems of each benchmark with each algorithm allotted 100 samples.

SampleSearch (IJGP-ss) [Gogate and Dechter, 2011], and Dynamic Importance Sampling [Lou et al., 2019]. Thus, superior performance against CTX schemes implicitly indicates competitiveness against these other methods.

Abstraction Quality of the QB Schemes. When drawing an equal number of samples with the same abstraction gran-

iB-5, t-300sec, Exact		DBN			Grids			Pedigree			Promedas			
Class	Scheme	nAbs	Fail	Avg. Error	Fail	Avg. Error	Fail							
QB	4	0	1.684	0	3.622	0	1.434	2	2.518	0	1.062	1	2.442	
	minVar	64	0	0.180	0	1.897	0	0.210	1	1.062	0	0.479	2	1.837
	1024	0	0.060	0	1.566	0	0.479	0	0.479	0	0.462	0	0.462	
	4	0	1.594	0	5.861	0	1.668	1	1.804	0	0.221	0	0.570	
	64	0	0.236	0	2.570	0	0.421	0	0.421	0	0.155	0	0.462	
	1024	0	0.051	0	1.844	0	0.479	0	0.479	0	0.155	0	0.462	
CTX	4	0	1.371	0	5.988	0	1.648	1	1.678	0	0.231	0	0.596	
	64	0	0.215	0	2.438	0	0.479	0	0.479	0	0.150	0	0.455	
	1024	0	0.150	0	1.891	0	0.479	0	0.479	0	0.150	0	0.455	
	4	0	1.381	0	5.030	0	1.852	7	4.643	0	0.596	1	2.442	
	64	0	1.763	0	5.950	0	1.114	0	1.114	0	0.479	0	0.479	
	1024	0	2.007	0	5.513	0	0.479	0	0.479	0	0.479	0	0.479	
RAND	4	0	1.850	0	5.933	0	1.332	10	5.729	0	0.479	0	0.479	
	64	0	3.510	0	4.021	0	0.479	6	4.349	0	0.479	0	0.479	
	1024	0	5.086	0	5.136	0	1.041	15	6.688	0	0.479	0	0.479	
	4	0	1.018	0	4.329	0	1.705	2	2.947	0	0.479	0	0.479	
	64	0	0.418	0	2.094	0	0.212	0	0.212	0	0.479	0	0.479	
	1024	0	0.120	0	1.501	0	0.143	0	0.143	0	0.479	0	0.479	

Table 5: Varying nAbs. Average error when using $nAbs \in \{4, 64, 1024\}$ for minVarQB, equalDistQB3, equalDistQB4, the CTX based algorithms, and RAND, each with iB-5 and time limit of 300 sec.

ularity of $nAbs = 256$ (Table 4), QB with *equalDist3* and *equalDist4* and RAND are well performing as seen when

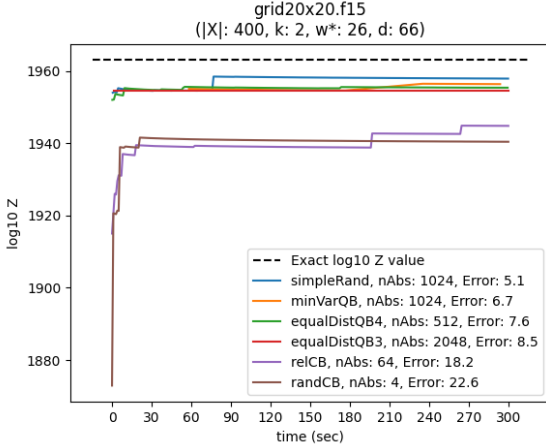


Figure 6: Z estimates from various algorithms versus time on Exact Grids problem grid20x20.f15 using $iB = 5$. The dashed black line shows the true Z value.

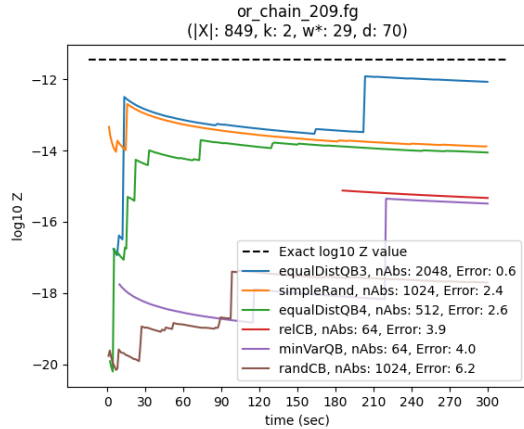


Figure 7: Z estimates from various algorithms versus time on Exact Promedas problem or_chain_209.fg using $iB = 5$. The dashed black line shows the true Z value.

using a time limit (Table 3). A key difference is that QB with *minVar*, which had showed slightly worse performance under a time limit, is now best. This in part explains the success of QB *equalDist3* and *equalDist4*, which try to emulate QB *minVar* while using faster greedy strategies.

Anytime Behavior. Figure 6 and Figure 7 show that Abstraction Sampling estimates continue to improve as time progresses. We also notice that estimates are often underestimates that increase over time, a common phenomenon of importance sampling due to the proposal distribution’s tails.

Choice of Abstraction Granularity. From Table 5 we see that for the well performing QB *equalDist3* and *equalDist4* schemes and for the RAND scheme there is a trend that greater *nAbs* improves performance. Figure 5 further supports this for QB with *equalDist4*, for which plots of QB *equalDist3* and RAND have similar profiles (omitted for brevity). However in Figure 4 and Table 5 we see that for *minVar* error begins to increase when *nAbs* becomes too high. This can be explained by the higher computational cost of forming *minVar* abstractions (which is more time

	HB	HRB	QB
simple	2.75	1.12	0.72
minVar	1.05	1.13	2.95
equalDist	0.75	0.59	1.16
equalDist2	0.84	0.75	1.82
equalDist3	1.20	1.01	4.05
equalDist4	0.87	1.14	3.90
rand	2.41	0.93	0.60

Figure 8: Performance Matrix. Relative average performance of value-based schemes vs. existing context-based abstractions. Values > 1.00 indicate superior performance.

consuming), leaving less time for probe generation.

Summary of Results. Experiments show the QB scheme with *equalDist3* or *equalDistQB4* and RAND performing the best of the newly proposed abstraction functions, significantly outperforming the former state-of-the-art (Figure 8). These schemes tend to improve as the abstraction granularity *nAbs* increases up to a point, past which we see little difference in performance. Thus, our study suggests that these three abstraction schemes should be the first choice when using AOAS, and be used with the largest *nAbs* feasible.

7 CONCLUSION

This exploration of abstraction functions for use with AND/OR Abstraction Sampling (AS) featured a new value-based abstraction framework, introducing three abstraction classes: HB, QB, and HRB each defined by real-valued functions that aim to capture informative elements from search and sampling to guide abstractions and improve AS performance. Each class was tested with each of seven node partitioning schemes to form twenty-one new abstraction functions. Additionally, a new purely randomized abstraction scheme, RAND, was presented that places nodes into equal cardinality abstract states completely at random.

Results from an extensive empirical evaluation on over 400 benchmark problems show two of the QB based schemes (*equalDistQB3*, and *equalDistQB4*) and the RAND scheme having superior performance consistently and throughout all benchmarks. In particular, performance was significantly improved relative to former state-of-the-art context-based abstractions, and thus also implicitly against Importance Sampling, Weighted Mini-Bucket Importance Sampling, IJGP-SampleSearch, and Dynamic Importance Sampling.

Based on this study and earlier findings, we believe that AOAS is one of the best schemes for estimating the partition function to date. Future work will explore adjusting the abstraction schemes to problem instances through learning and also the potential for applying adaptive sampling.

Acknowledgements

Thank you to the reviewers for their valuable comments and suggestions. This work was supported in part by NSF grants IIS-2008516 and CNS-2321786.

References

- Filjor Broka, Rina Dechter, Alexander Ihler, and Kalev Kask. Abstraction sampling in graphical models. In *Proceedings of the Thirty-Fourth Conference on Uncertainty in Artificial Intelligence, UAI 2018, Monterey, California, USA, August 6-10, 2018*, pages 632–641, 2018. URL <http://auai.org/uai2018/proceedings/papers/234.pdf>.
- P.-C. Chen. Heuristic sampling: A method for predicting the performance of tree searching programs. *SIAM Journal on Computing*, 21:295–315, 1992.
- A. Darwiche. *Modeling and Reasoning with Bayesian Networks*. Cambridge University Press, 2009.
- Rina Dechter. *Reasoning with Probabilistic and Deterministic Graphical Models: Exact Algorithms*. Synthesis Lectures on Artificial Intelligence and Machine Learning. Morgan & Claypool Publishers, 2013. doi: 10.2200/S00529ED1V01Y201308AIM023. URL <http://dx.doi.org/10.2200/S00529ED1V01Y201308AIM023>.
- Rina Dechter and Robert Mateescu. AND/OR search spaces for graphical models. *Artificial Intelligence*, 171(2-3):73–106, 2007.
- Rina Dechter and Irina Rish. Mini-buckets: A general scheme for bounded inference. *J. ACM*, 50(2):107–153, 2003. doi: 10.1145/636865.636866. URL <http://doi.acm.org/10.1145/636865.636866>.
- Vibhav Gogate and Rina Dechter. Samplesearch: Importance sampling in presence of determinism. *Artif. Intell.*, 175(2):694–729, 2011. doi: 10.1016/j.artint.2010.10.009. URL <https://doi.org/10.1016/j.artint.2010.10.009>.
- Vincent Hsiao, Dana Nau, and Rina Dechter. Graph neural networks for dynamic abstraction sampling. In *AAAI Workshop on Graphs and More Complex Structures for Learning and Reasoning (GCLR)*, 2023.
- Alexander Ihler, Natalia Flerova, Rina Dechter, and Lars Otten. Join-graph based cost-shifting schemes. In Nando de Freitas and Kevin P. Murphy, editors, *Proceedings of the Twenty-Eighth Conference on Uncertainty in Artificial Intelligence, Catalina Island, CA, USA, August 14-18, 2012*, pages 397–406. AUAI Press, 2012. URL https://dslpitt.org/uai/displayArticleDetails.jsp?mmnu=1&smnu=2&article_id=2302&proceeding_id=28.
- Kalev Kask, Bobak Pezeshki, Filjor Broka, Alexander Ihler, and Rina Dechter. Scaling up and/or abstraction sampling. In Christian Bessiere, editor, *Proceedings of the Twenty-Ninth International Joint Conference on Artificial Intelligence, IJCAI-20*, pages 4266–4274. International Joint Conferences on Artificial Intelligence Organization, 7 2020. doi: 10.24963/ijcai.2020/589. URL <https://doi.org/10.24963/ijcai.2020/589>. Main track.
- D.E. Knuth. Estimating the efficiency of backtracking algorithms. *Math. Comput.*, 29:1121–136, 1975.
- G. N. Lance and W. T. Williams. A General Theory of Classificatory Sorting Strategies: 1. Hierarchical Systems. *The Computer Journal*, 9(4):373–380, 02 1967. ISSN 0010-4620. doi: 10.1093/comjnl/9.4.373. URL <https://doi.org/10.1093/comjnl/9.4.373>.
- Qiang Liu and Alexander Ihler. Bounding the partition function using holder’s inequality. In *Proceedings of the 28th International Conference on Machine Learning, ICML 2011, Bellevue, Washington, USA, June 28 - July 2, 2011*, pages 849–856, 2011.
- Qiang Liu, John W Fisher III, and Alexander Ihler. Probabilistic variational bounds for graphical models. In C. Cortes, N. D. Lawrence, D. D. Lee, M. Sugiyama, and R. Garnett, editors, *Advances in Neural Information Processing Systems 28*, pages 1432–1440. Curran Associates, Inc., 2015.
- Qi Lou, Rina Dechter, and Alexander Ihler. Interleave variational optimization with monte carlo sampling: A tale of two approximate inference paradigms. 2019.
- R. Marinescu and Rina Dechter. Memory intensive AND/OR search for combinatorial optimization in graphical models. *Artificial Intelligence*, 173(16-17):1492–1524, 2009.
- Robert Mateescu and Rina Dechter. The relationship between and/or search and variable elimination. pages 380–387, 01 2005.
- J. Pearl. *Probabilistic Reasoning in Intelligent Systems*. Morgan Kaufmann, 1988.
- Maria L. Rizzo. *Statistical computing with R*. Chapman & Hall/CRC, 2007.
- Reuven Y. Rubinstein and Dirk P. Kroese. *Simulation and the Monte Carlo Method*. Wiley Publishing, 3rd edition, 2016. ISBN 1118632168.
- Joe H. Ward. Hierarchical grouping to optimize an objective function. *Journal of the American Statistical Association*, 58(301):236–244, 1963. ISSN 01621459. URL <http://www.jstor.org/stable/2282967>.

Value-Based Abstraction Functions for Abstraction Sampling

(Supplemental Materials)

Bobak Pezeshki¹

Kalev Kask¹

Alexander Ihler¹

Rina Dechter¹

¹University of California, Irvine

Abstract

For revised supplemental materials, please visit <https://ics.uci.edu/~dechter/publications.html>. This document includes supplemental background, descriptions, details, and results in extension to the main paper. Given its size, we suggest using the table of contents to navigate. For an additional background on graphical models, AND/OR search trees, and variable elimination, please view the EXTENDED BACKGROUND supplemental document.

CONTENTS

1 AOAS Background	3
1.1 Sample Algorithm Trace	3
1.2 Detailed Algorithm	3
2 Probe Size Variability	5
3 Exact Abstraction Proofs	7
3.1 ORAS	7
3.2 AOAS	8
4 Paradigms Intuiting Abstraction Strategies	10
4.1 Search Paradigms	10
4.2 Sampling Paradigms	10
5 Additional Information About Value-Based Abstractions	12
6 Detailed Descriptions of Ordered Partitioning Schemes for Value Based Abstractions	13
6.0.1 simpleVB	13
6.0.2 minVarVB	14
6.0.3 equalDistVB	15

6.0.4	equalDistVB2	16
6.0.5	equalDistVB3	17
6.0.6	equalDistVB4	17
6.0.7	randVB	18
7	Extended Results	19
7.1	Summary Comparison.	19
7.1.1	Exact Problems	19
7.1.2	LARGE Problems	21
7.2	Comparison using 100 Samples.	23
7.2.1	Exact Problems	23
7.2.2	LARGE Problems	23
7.3	Time Series Plot	24
7.3.1	LARGE Problems	24
8	Additional Results	28
8.1	Probe Size	28
8.2	Abstraction Speed	28

1 AOAS BACKGROUND

Taken with permission directly from Kask et al. [2020].

1.1 SAMPLE ALGORITHM TRACE

Here we show a trace of abstraction sampling using the AOAS algorithm using an abstraction function that groups AND nodes of the same domain value together in an abstract state.

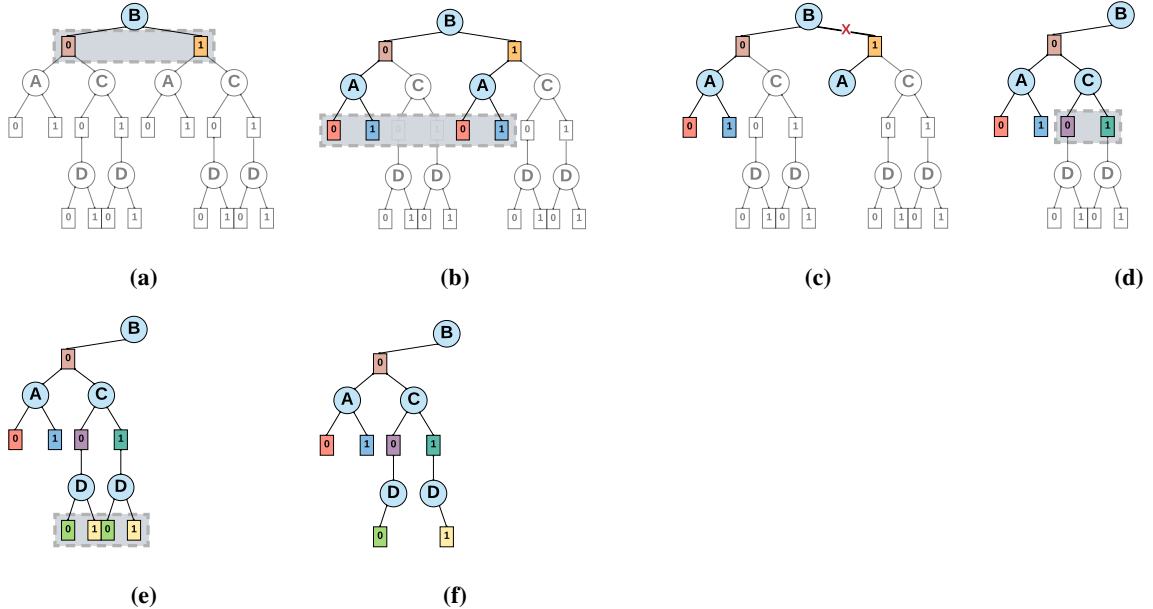


Figure 1: From Kask et al. [2020], a sample trace of AOAS following DFS ordering $B \rightarrow A \rightarrow C \rightarrow D$. Transparent nodes indicate portions of the reachable search space yet to be explored. Gray boxes indicate nodes considered for abstraction. Nodes with the same domain values (also indicated by the same color) are abstracted into the same abstract state. Only one node of each color is stochastically selected as a representative for its respective abstract state. Step (c) shows an optional optional pruning step. Step (f) shows the final example probe capturing four full configurations: $B = 0, A = 0, C = 0, D = 0, B = 0, A = 1, C = 0, D = 0, B = 0, A = 0, C = 1, D = 1, B = 0, A = 1, C = 1, D = 1$.

Starting with variable B (Figure 1a), each node belongs to a different abstraction and is therefore kept. Next, we expand to A and abstract across its nodes (Figure 1b). Not restricted to *proper* abstractions, we partition across *all* nodes of A , regardless of whether they fall under $B=0$ or $B=1$. We see two nodes in each abstract state (denoted by the red and blue coloring). Next we calculate their respective proposals (line 21). Note that the proposal of each node n relies on $r(n)$ (line 15), which captures the values of the nodes in its $Out(path(n))$, in this case nodes of C . Since the nodes of C have not been expanded yet, we use their heuristic values as an approximation of their values. We then stochastically choose a representative from each abstract state (line 23). Suppose that both red and blue representatives are stochastically chosen from under $B=0$ (Figure 1c). Since A has no descendant, we backtrack to B , updating its node values (line 33) and performing a pruning step (line 31). In pruning, we remove AND nodes of B that do not extend to AND nodes of A , and thus prune $B=1$ (denoted by the red "X" in Figure 1c), in order to ensure formation of proper AND/OR probes. Finally, we expand and abstract C and D (Figures 1d-1f). The $r(n)$ for D 's nodes is inherited from the $r(n_C)$ of its respective n_C parent. We backtrack from D to the root updating values (no further pruning was necessary). The result is a valid probe (Figure 1f) containing four solutions: $(B=0, A=0, C=0, D=0)$, $(B=0, A=0, C=1, D=1)$, $(B=0, A=1, C=0, D=0)$, and $(B=0, A=1, C=1, D=1)$. We estimate the partition function by computing $\hat{Z}(B)$.

1.2 DETAILED ALGORITHM

Algorithm 1: AOAS.

Input: Graphical model $\mathcal{M} = (\mathbf{X}, \mathbf{D}, \Phi)$, a pseudo tree \mathcal{T} for \mathcal{M} rooted at a dummy singleton variable D , an abstraction function a , heuristic function h . For any node n , $g(n) =$ its path cost, $w(n) =$ its importance weight, and $\hat{Z}(n) =$ its estimated value (initialized to $h(n)$).
Output: $\hat{Z}_{\mathcal{M}}$, an estimate of the partition function of \mathcal{M}

```

1 Function AOAS ( $\mathcal{T}, h, a$ )
2 begin
3    $PROBE \leftarrow n_D, g(n_D), w(n_D), r(n_D), \hat{Z}(n_D) \leftarrow 1$ 
4    $STACK \leftarrow push(\text{empty stack}, D)$ 
5   while  $STACK$  is not empty do
6      $X \leftarrow top(STACK)$ 
7     if  $X$  has unvisited children in  $\mathcal{T}$  then
8        $Y \leftarrow$  the next unvisited child of  $X$ 
9       foreach  $n_X \in PROBE$  do
10       $PROBE \leftarrow PROBE$  expanded from  $n_X$  to  $Y$ 
11       $F'_Y \leftarrow$  newly added AND nodes of  $Y \in PROBE$ 
12      foreach  $n_Y \in F'_Y$  do
13         $w(n_Y) \leftarrow w(n_X)$ 
14         $g(n_Y) \leftarrow g(n_X) \cdot c(n_Y)$ 
15         $r(n_Y) \leftarrow r(n_X) \cdot \prod_{\{S \neq Y \in ch_{\mathcal{T}}(X)\}} \hat{V}(S_{n_X})$ 
16      end
17    end
18     $A \leftarrow \{A_i \mid A_i = \{n_Y \in PROBE \mid a(n)=i\}\}$ 
19    foreach  $A_i \in A$  do
20      foreach  $n \in A_i$  do
21         $p(n) \leftarrow \frac{w(n) \cdot g(n) \cdot h(n) \cdot r(n)}{\sum_{m \in A_i} w(m) \cdot g(m) \cdot h(m) \cdot r(m)}$ 
22      end
23       $n_{Y_i} \propto_p A_i$ ;  $//$  randomly select
24       $w(n_{Y_i}) \leftarrow w(n_{Y_i}) / p(n_{Y_i})$ 
25       $\hat{Z}(n_{Y_i}) \leftarrow 1$ 
26       $PROBE \leftarrow PROBE \setminus A_i \cup \{n_{Y_i}\}$ 
27    end
28     $push(STACK, Y)$ 
29  else
30     $pop(STACK), W \leftarrow top(STACK)$ 
31     $PROBE \leftarrow PROBE$  s.t. all  $n_W$  without descendants are pruned
32    foreach  $n_W$  in  $PROBE$  do
33       $\hat{Z}(n_W) \leftarrow \hat{Z}(n_W) \cdot \sum_{n_X \leftarrow child(n_W)} \hat{Z}(n_X) \cdot c(n_X) \cdot \frac{w(n_X)}{w(n_W)}$ 
34    end
35    if  $X = D$  then  $\hat{Z}_{\mathcal{M}} = \hat{Z}(D)$ ;
36  end
37 end
38 return  $\hat{Z}_{\mathcal{M}}$ 
39 end

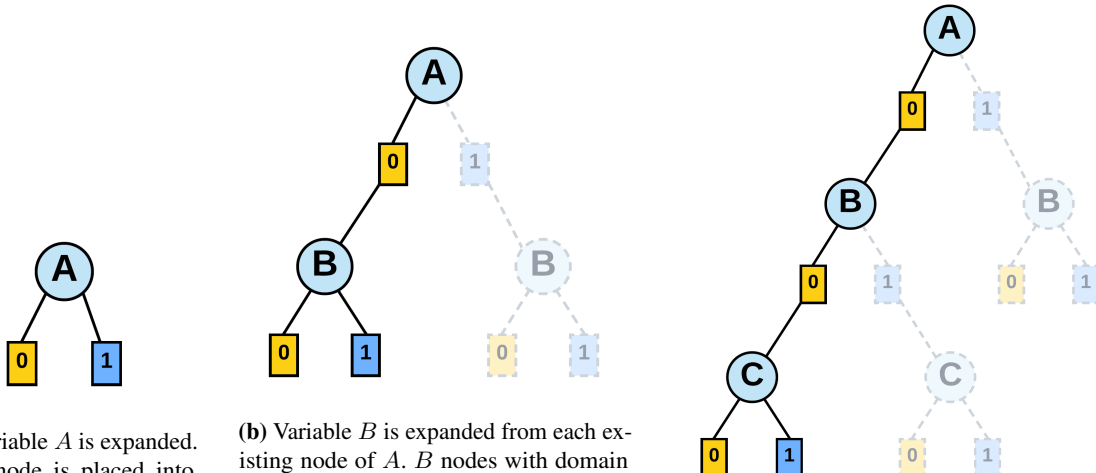
```

2 PROBE SIZE VARIABILITY

Even with the same abstraction function and granularity (ie. allowed number of abstract states per level), probe sizes can vary greatly. One reason for this is due to abstractions causing nodes from certain branches of the probe to be replaced by representative from other branch, and thus the current branch will no longer be extended. We provide a paired example in Figure 3 and Figure 4 where in both cases the probes are constructed according to the pseudo tree shown in Figure 2, an abstraction function is used that groups nodes with the same domain value together (indicated by yellow coloring for grouping of nodes with a domain value of 0 and blue coloring grouping nodes together that have domain value of 1) is used, and the abstraction granularity is set to $nAbs = 2$ (meaning that nodes are abstracted into at most two abstract states).



Figure 2: A linear psuedo tree.

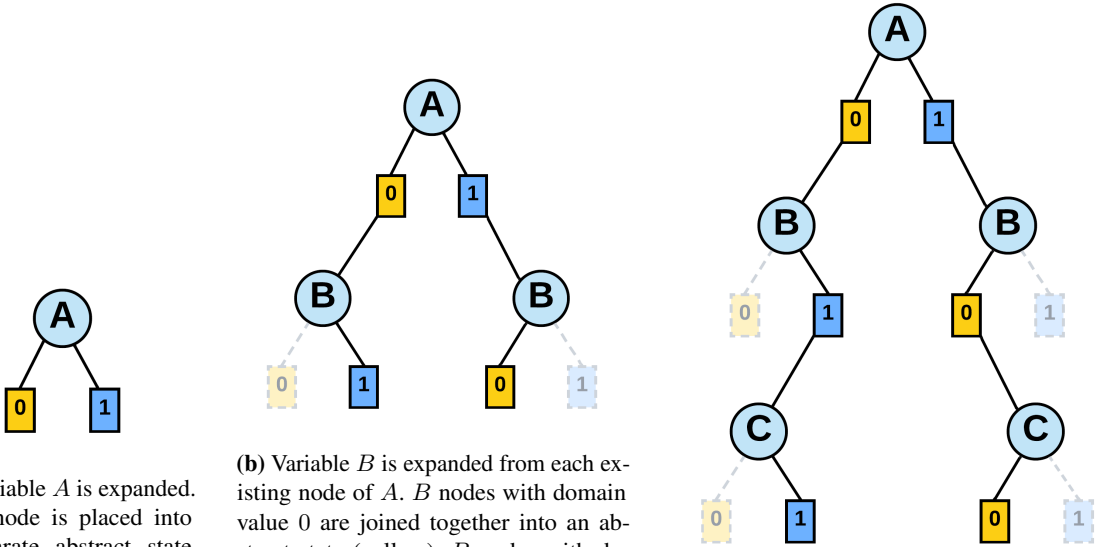


(a) Variable A is expanded. Each node is placed into a separate abstract state and each is selected to represent their respective abstract state.

(b) Variable B is expanded from each existing node of A . B nodes with domain value 0 are joined together into an abstract state (yellow); B nodes with domain value 1 constitute a different abstract state (blue). For each resulting abstract state, the corresponding node underneath the branch of $A \leftarrow 0$ is stochastically selected as the representative. As there are no selected representatives underneath the branch of $A \leftarrow 1$, those nodes will no longer be extended (and can be pruned).

(c) Variable C is expanded from each representative node of B . C nodes with domain value 0 are joined together into an abstract state (yellow); C nodes with domain value 1 constitute a different abstract state (blue). For each resulting abstract state, the corresponding node underneath the branch of $A \leftarrow 0, B \leftarrow 0$ is stochastically selected as the representative. As there are no selected representatives underneath the branch of $A \leftarrow 0, B \leftarrow 1$, those nodes will no longer be extended (and can be pruned).

Figure 3: An example of a "skewed" probe construction following the pseudo tree in Figure 2, using an abstraction function that groups nodes of the same domain value into the same abstract state, and using a granularity of $nAbs = 2$. At each level, representatives of all abstract states are chosen under the same single branch, thus only extending only one path in the probe.



(a) Variable A is expanded. Each node is placed into a separate abstract state and each is selected to represent their respective abstract state.

(b) Variable B is expanded from each existing node of A . B nodes with domain value 0 are joined together into an abstract state (yellow); B nodes with domain value 1 constitute a different abstract state (blue). The stochastically selected representative from the $B = 1$ abstract state ends up under the $A \leftarrow 0$ branch while the representative from the $B = 0$ abstract state is selected from under $A \leftarrow 1$. As a result, both $A \leftarrow 0$ and $A \leftarrow 1$ branches have an extension to a node from B and will continue to be extended.

(c) Variable C is expanded from each existing node of B . C nodes with domain value 0 are joined together into an abstract state (yellow); C nodes with domain value 1 constitute a different abstract state (blue). The stochastically selected representative from the $C = 1$ abstract state ends up under the $A \leftarrow 0, B \leftarrow 1$ branch while the representative from the $C = 0$ abstract state is selected from under $A \leftarrow 1, B \leftarrow 0$. As a result, both $A \leftarrow 0, B \leftarrow 1$ and $A \leftarrow 1, B \leftarrow 0$ branches have an extension to a node from C and will continue to be extended.

Figure 4: An example of a "balanced" probe construction following the pseudo tree in Figure 2, using an abstraction function that groups nodes of the same domain value into the same abstract state, and using a granularity of $nAbs = 2$. At each level, representatives of all abstract states are chosen under the same single branch, thus only extending only one path in the probe.

3 EXACT ABSTRACTION PROOFS

Required Definitions.

Definition 3.0.0.1 (Abstraction Function $h(n)$ vs. $Z(n)$ Proportionality)
An abstraction function $a(n)$ maintains $h(n)$ vs. $Z(n)$ proportionality if, for every abstract state A_i formed by $a(n)$, $\forall n \in A_i, h(n) = \alpha Z(n)$, for some constant α specific to A_i .

Definition 3.0.0.2 (Abstraction Function $h(n)r(n)$ vs. $Z(n)R(n)$ Proportionality)
An abstraction function $a(n)$ maintains $h(n)r(n)$ vs. $Z(n)R(n)$ proportionality if, for every abstract state A_i formed by $a(n)$, $\forall n \in A_i, h(n)r(n) = \alpha Z(n)R(n)$, for some constant α specific to A_i .

Definition 3.0.0.3 (Exact Abstraction Function)
An abstraction function $a(\cdot)$ is exact for an abstraction sampling algorithm, AS, if use of $a(\cdot)$ with AS always leads to AS estimates having zero variance and $\hat{Z} = Z$ for every AS probe.

3.1 ORAS

Theorem 3.1.0.1 (ORAS Exact Abstractions from $h(n)$ vs. $Z(n)$ Proportionality)

If an abstraction function $a(\cdot)$ maintains $h(n)$ vs. $Z(n)$ Proportionality, then it is an exact abstraction function for ORAS.

Proof. We know that if we were to use exhaustive search, we would arrive at the true Z value. We use a proof by induction that assumes that after each abstraction step we will compute the rest of the probe exactly using exhaustive search. Thus, if abstractions are performed layer by layer down from the root, after each abstraction we know that $Z(n')$ will be computed exactly for the selected node n' .

We denote the estimate that would be generated by a probe constructed after t time steps as $\hat{Z}^{(t)}(\text{PROBE})$. (As we will describe, each time step will correspond to an abstraction step). As a base case, $\hat{Z}^{(t=0)}(\text{PROBE}) = Z$ since all values will be computed exactly via exhaustive search. In the inductive step, we will show that after each time step t , if instead of using exhaustive search immediately, we first perform an abstraction on the current level of the probe, the resulting estimate of the newly abstracted probe $\hat{Z}^{(t+1)}(\text{PROBE})$ will remain unchanged. Namely, we will show that

$$\hat{Z}^{(t)}(\text{PROBE}) - \hat{Z}^{(t+1)}(\text{PROBE}) = 0$$

This shows that the abstractions maintain exactness of the probe's estimate.

Starting from the left hand side

$$LHS = \hat{Z}^{(t)}(\text{PROBE}) - \hat{Z}^{(t+1)}(\text{PROBE})$$

We note the difference in the overall probe estimates during an Abstraction Sampling is due to the change in the probe estimate that results from each individual abstraction step (namely selection and reweighing of a representative node n' from an abstract state A_i). Thus for our time steps, we will focus on the difference in value resulting from a single arbitrary abstraction step.

$$= \sum_{n \in A_i} w^{(t)}(n)g(n)Z(n) - w^{(t+1)}(n')g(n')Z(n')$$

Above, the left term shows the contribution to the partition function due to nodes of abstract state A_i (still assuming we will perform exhaustive search below each one), and the right term is the contribution of a selected node n' after abstraction (note the adjustment to the selected node's weight).

Using the fact that $w^{(t+1)}(n') = \frac{w^{(t)}(n')}{p(n')}$ (from the importance weight modification), we now get

$$= \sum_{n \in A_i} w^{(t)}(n)g(n)Z(n) - \frac{w^{(t)}(n')}{p(n')}g(n')Z(n')$$

(Note that $p(n')$ cannot be zero, otherwise n' would not have been selected).

Noting that for $p(n') = \frac{w^{(t)}(n')g(n')h(n')}{\sum_{n \in A_i} w^{(t)}(n)g(n)h(n)}$ and substituting we get

$$\begin{aligned} &= \sum_{n \in A_i} w^{(t)}(n)g(n)Z(n) \\ &\quad - w^{(t)}(n')g(n')Z(n') \frac{\sum_{n \in A_i} w^{(t)}(n)g(n)h(n)}{w^{(t)}(n')g(n')h(n')} \\ &= \sum_{n \in A_i} w^{(t)}(n)g(n)Z(n) - \frac{Z(n')}{h(n')} \sum_{n \in A_i} w^{(t)}(n)g(n)h(n) \end{aligned}$$

Now, per our assumption, $\forall n \in A_i$, let $h(n) = \alpha Z(n)$, where α is the proportionality constant by which $h(n)$ differs from $Z(n)$. Then

$$\begin{aligned} &= \sum_{n \in A_i} w^{(t)}(n)g(n)Z(n) - \frac{Z(n')}{\alpha Z(n')} \sum_{n \in A_i} w^{(t)}(n)g(n)\alpha Z(n) \\ &= \sum_{n \in A_i} w^{(t)}(n)g(n)Z(n) - \frac{\alpha}{\alpha} \sum_{n \in A_i} w^{(t)}(n)g(n)Z(n) \\ &= \sum_{n \in A_i} w^{(t)}(n)g(n)Z(n) - \sum_{n \in A_i} w^{(t)}(n)g(n)Z(n) \\ &= 0 = RHS \end{aligned}$$

□

□

3.2 AOAS

Theorem 3.2.0.1 (AOAS Exact Abstractions from $h(n)r(n)$ vs. $Z(n)R(n)$ Proportionality)

If an abstraction function $a(\cdot)$ maintains $h(n)r(n)$ vs. $Z(n)R(n)$ Proportionality, then it is an exact abstraction function for AOAS.

Proof. We know that if we were to use exhaustive search, we would arrive at the true Z value. We use a proof by induction that assumes that after each abstraction step we will compute the rest of the probe exactly using exhaustive search. Thus, if abstractions are performed layer by layer down from the root, after each abstraction we know that $Z(n')$ will be computed exactly for the selected node n' . We also assume that, $R(n)$ for every node will be computed exactly. This assumption holds true before we perform any abstractions (as everything is computed exactly via exhaustive search) and continues to hold if we can show that, after each abstraction step, the resulting estimates remains unchanged (and thus remains exact).

We denote the estimate that would be generated by a probe constructed after t time steps as $\hat{Z}^{(t)}(\text{PROBE})$. (As we will describe, each time step will correspond to an abstraction step). As a base case, $\hat{Z}^{(t=0)}(\text{PROBE}) = Z$ since all values will be computed exactly via exhaustive search. In the inductive step, we will show that after each time step t , if instead of using exhaustive search immediately, we first perform an abstraction on the current level of the probe, the resulting estimate of the newly abstracted probe $\hat{Z}^{(t+1)}(\text{PROBE})$ will remain unchanged. Namely, we will show that

$$\hat{Z}^{(t)}(\text{PROBE}) - \hat{Z}^{(t+1)}(\text{PROBE}) = 0$$

This shows that the abstractions maintain exactness of the probe's estimate.

Starting from the left hand side

$$LHS = \hat{Z}^{(t)}(\text{PROBE}) - \hat{Z}^{(t+1)}(\text{PROBE})$$

We note the difference in the overall probe estimates during an Abstraction Sampling is due to the change in the probe estimate that results from each individual abstraction step (namely due to the selection and reweighing of a representative node n' from an abstract state A_i). Thus for our time steps, we will focus on the difference in value resulting from a single arbitrary abstraction step.

$$= \sum_{n \in A_i} w^{(t)}(n)g(n)Z(n)R(n) - w^{(t+1)}(n')g(n')Z(n')R(n')$$

Above, the left term shows the contribution to the partition function due to nodes of abstract state A_i (still assuming we will perform exhaustive search below each one), and the right term is the contribution of a selected node n' after abstraction (note the adjustment to the selected node's weight).

Using the fact that $w^{(t+1)}(n') = \frac{w^{(t)}(n')}{p(n')}$ (from the importance weight modification), we now get

$$= \sum_{n \in A_i} w^{(t)}(n)g(n)Z(n)R(n) - \frac{w^{(t)}(n')}{p(n')}g(n')Z(n')R(n')$$

(Note that $p(n')$ cannot be zero, otherwise n' would not have been selected).

Noting that for $p(n') = \frac{w^{(t)}(n')g(n')h(n')r(n')}{\sum_{n \in A_i} w^{(t)}(n)g(n)h(n)r(n)}$ and substituting we get

$$\begin{aligned} &= \sum_{n \in A_i} w^{(t)}(n)g(n)Z(n)R(n) \\ &\quad - w^{(t)}(n')g(n')Z(n')R(n') \frac{\sum_{n \in A_i} w^{(t)}(n)g(n)h(n)r(n)}{w^{(t)}(n')g(n')h(n')r(n')} \\ &= \sum_{n \in A_i} w^{(t)}(n)g(n)Z(n)R(n) \\ &\quad - \frac{Z(n')R(n')}{h(n')r(n')} \sum_{n \in A_i} w^{(t)}(n)g(n)h(n)r(n) \end{aligned}$$

Now, per our assumption, $\forall n \in A_i$, let $h(n)r(n) = \alpha Z(n)R(n)$, where α is the proportionality constant by which $h(n)r(n)$ differs from $Z(n)R(n)$. Then

$$\begin{aligned} &= \sum_{n \in A_i} w^{(t)}(n)g(n)Z(n)R(n) \\ &\quad - \frac{Z(n')R(n')}{\alpha Z(n')R(n')} \sum_{n \in A_i} w^{(t)}(n)g(n) \alpha Z(n)R(n) \\ &= \sum_{n \in A_i} w^{(t)}(n)g(n)Z(n)R(n) \\ &\quad - \frac{\alpha}{\alpha} \sum_{n \in A_i} w^{(t)}(n)g(n)Z(n)R(n) \\ &= \sum_{n \in A_i} w^{(t)}(n)g(n)Z(n)R(n) - \sum_{n \in A_i} w^{(t)}(n)g(n)Z(n)R(n) \\ &= 0 = RHS \end{aligned}$$

□

□

4 PARADIGMS INTUITING ABSTRACTION STRATEGIES

Next we review concepts from search and sampling that offer paradigms from which we draw ideas for abstraction functions.

4.1 SEARCH PARADIGMS

In [tree] search, one can merge nodes that have the same value to produce a more efficient graph search [Mateescu et al. \[2008\]](#). Abstraction functions by [Broka et al. \[2018\]](#) focused on this paradigm and approached it by using the concept of a node's context - the assignments to the smallest subset of a node's ancestor variables that dictates its value. Due to the potentially large context size for variables, and consequently the exponentially high number of combinations of assignments to the context, the full context of variables could not be used in most cases. [Broka et al. \[2018\]](#) resolved this by creating two context-based abstraction functions that were relaxed to allow nodes with different contexts to be grouped in the same abstract state. However, sharing the same partial context does not necessarily imply the same, nor even similar, node values. Our new Heuristic-Based abstractions hope to provide more accurate abstractions based on the same ideology.

4.2 SAMPLING PARADIGMS

Consider wanting to compute the $\mathbb{E}_{p^*}[f(x)] = \sum_x f(x)p^*(x)$ for a distribution $p^*(.)$ over a variable X that is difficult to sample from but easy to evaluate, and given a positive value function $f(x)$. Using a proposal distribution $p(.)$ that is easy to sample from, and noticing the equivalency of the target quantity with $\sum_x \frac{f(x)p^*(x)}{p(x)}p(x)$, we can estimate the quantity by importance sampling by drawing m samples to estimate the equivalent quantity $\mathbb{E}_p[f(x)\frac{p^*(x)}{p(x)}] \approx \frac{1}{m} \sum_{j=1}^m f(x^{(j)})\frac{p^*(x^{(j)})}{p(x^{(j)})}, x^{(j)} \sim p$. It is well known that importance sampling achieves zero variance when 1) $p(x) = 0 \implies p^*(x) = 0$, and 2) otherwise $p(x)$ is proportional to $p^*(x)f(x)$ [Kahn and Marshall \[1953\]](#), [Owen \[2013\]](#).

Lemma 4.2.0.1 (Importance Sampling Exact Proposal Based on Proportionality with Target Distribution)

Given a distribution $p^(.)$ over a variable X that is easy to evaluate, and given a positive value function $f(x)$, importance sampling to estimate $\mathbb{E}_{p^*}[f(x)]$ achieves zero variance when using a proposal function $p(.)$ such that 1) $p(n) = 0 \implies p^*(n)f(n) = 0$, and 2) $p(n) \propto p^*(n)f(n)$, otherwise.*

Note that we can also use importance sampling to simply compute $\sum_x f(x) = \sum_x \frac{f(x)}{p(x)}p(x) = \mathbb{E}_p[\frac{f(x)}{p(x)}] \approx \frac{1}{m} \sum_{j=1}^m \frac{f(n^{(j)})}{p(x^{(j)})}, x^{(j)} \sim p$. Note that the partition function over a graphical model, $Z = \sum_{\mathbf{x}} \mathbf{F}(\mathbf{x}), \mathbf{F}(\mathbf{x}) = \prod_{f \in \mathbf{F}} f(x)$, has the form of this task.

In fact, expanding an AND/OR search tree level-by-level, the partition function Z with respect to the nodes n at any variable X can be written as $Z = \sum_n g(n)Z(n)R(n)$. Thus, using a proposal $p(.)$ to perform importance sampling at any level we could instead estimate

$$Z = \sum_n g(n)Z(n)R(n) = \sum_x \frac{g(n)Z(n)R(n)}{p(n)}p(n) \quad (1)$$

$$\approx \frac{1}{m} \sum_{j=1}^m \frac{g(n^{(j)})Z(n^{(j)})R(n^{(j)})}{p(n^{(j)})}, n^{(j)} \sim p \quad (2)$$

Thus, sampling at any level would also allow for zero variance / exact computation if similarly $p(n) \propto g(n)Z(n)R(n)$.

Note that in Abstraction Sampling each abstract state involves a node selection procedure analogous to importance sampling and that AOAS uses a proposal $p(n) \propto g(n)h(n)r(n)$. $g(n)$ can always be evaluated exactly. Then assuming that $h(n) = 0 \implies Z(n) = 0$ and $r(n) = 0 \implies R(n) = 0$, it naturally follows that designing each abstract states A_i such that $\forall n \in A_i, h(n)r(n) = \alpha g(n)Z(n)R(n)$, for some constant α , we similarly achieve zero variance.

Definition 4.2.0.1 (Abstraction Function $h(n)r(n)$ vs. $Z(n)R(n)$ Proportionality)

An abstraction function $a(n)$ maintains $h(n)r(n)$ vs. $Z(n)R(n)$ proportionality if, for every abstract state A_i formed by $a(n)$, $\forall n \in A_i, h(n)r(n) = \alpha Z(n)R(n)$, for some constant α specific to A_i .

Definition 4.2.0.2 (Exact Abstraction Function)

An abstraction function $a(.)$ is exact for an abstraction sampling algorithm, AS, if use of $a(.)$ with AS always leads to AS estimates having zero variance and $\hat{Z} = Z$ for every AS probe.

Thus, we can say:

Theorem 4.2.0.2 (AOAS Exact Abstractions from $h(n)r(n)$ vs. $Z(n)R(n)$ Proportionality)

If an abstraction function $a(\cdot)$ maintains $h(n)r(n)$ vs. $Z(n)R(n)$ Proportionality, then it is an exact abstraction function for AOAS. (Proof in Supplemental Materials)

Normally we neither have access to the proportionality constant α or even know whether nodes have the same α . However one idea is to use the magnitude of $h(n)r(n)$ itself as a heuristic for similarities in α . This drives the intuition for a new HR-Based class of abstractions.

Also from a sampling perspective, [Rizzo \[2007\]](#) showed the following about stratified importance sampling when sampling from equal area strata under the proposal:

Proposition 4.2.0.3 (Stratified Importance Sampling Variance Reduction)

Suppose that $M = mk$ is the number of replicates for an importance sampling estimator $\hat{\theta}^I$, and $\hat{\theta}^{SI}$ is a stratified importance sampling estimator, with estimates $\hat{\theta}_j$ for θ_j on the individual strata, each with m replicates. If $Var(\hat{\theta}^I) = \sigma^2/M$ and $Var(\hat{\theta}_j) = \sigma_j^2/m$, $j = 1, \dots, k$, then

$$\sigma^2 - k \sum_{j=1}^k \sigma_j^2 \geq 0, \quad (3)$$

with equality if and only if $\theta_1 = \dots = \theta_k$. Hence stratification never increases variance, and there exists a stratification that reduces the variance except when [the proposal function] $g(x)$ is constant.

Two takeaways from this proposition are that 1) we can achieve variance reduction with respect to importance sampling (analogous to Abstraction Sampling with all nodes placed into a single abstract state) by stratifying into equal area strata under the proposal, and 2) reducing the variance of each strata σ_j^2 leads to greater variance reduction. These will help drive the intuition for a new Q-Based abstraction class, as well as motivate several new partitioning schemes.

5 ADDITIONAL INFORMATION ABOUT VALUE-BASED ABSTRACTIONS

As described in the main paper, value-based abstraction functions consist of two parts: (1) a value function $\mu : n \rightarrow \mathbb{R}$ that assigns a real value on a positive scale to nodes n that are to be abstracted, and (2) a partitioning scheme that then abstracts nodes based on $\mu(n)$. And because $\mu(n)$ are values on a positive scale (implying semantics between smaller vs. larger values), the partitioning schemes can be designed to partition the nodes in a way that maintains an ordering of $\mu(n)$. This results in what we call value-based ordered abstractions.

Algorithm 2: General Value-0Ordered Abstraction Function Scheme

input :A set of nodes n to be partitioned into abstract states; an abstraction value function $\mu(\cdot)$; a parameter $nAbs$ bounding the number of abstract states; a partitioning function $\Psi_o(\cdot)$ that partitions n into abstract states such that nodes are ordered by $\mu(n)$ according to sort-order o

output :Nodes n partitioned into abstract states $A = \{A_i \mid i \leq nAbs\}$ such that sort order o of $\mu(n)$ is maintained across all A_i .

```

1 begin
2   if |n| <= nAbs then
3     | A = {{n} | n in n}
4   else
5     | A = Psi_o(n, mu, nAbs)
6   return A
7 end

```

6 DETAILED DESCRIPTIONS OF ORDERED PARTITIONING SCHEMES FOR VALUE BASED ABSTRACTIONS

We now present seven schemes, each defined by a unique sort order o and partition strategy Ψ combination. Each scheme uses a different method to partition nodes into abstract states keeping the nodes in sort order according to o . With a provided value function $\mu(\cdot)$, each scheme can be used to form an ordered value abstraction function. In addition to defining each scheme, we also describe the motivation behind its creation.

Running Example As we motivate and describe the schemes, we will also provide an example of abstract states that would result from partitioning the following nodes:

$$\{1.0, 1.1, 1.2, 1.3, 1.4, 1.5, 10, 100\} \quad (4)$$

into $nAbs = 4$ abstract states by each of partitioning schemes that will be presented.

6.0.1 simpleVB

$\Psi_{simpleVB}$ (Algorithm 3)

Algorithm 3: $\Psi_{simpleVB}$

```

input : A set of nodes  $\mathbf{n}$  to be partitioned into  $nAbs$  abstract states; a value function  $\mu(\cdot)$ 
output :  $\mathbf{n}$  partitioned into abstract states1  $\mathbf{A} = \{\mathbf{A}_i \mid i \in \{1, \dots, nAbs\}\}$  such that  $\forall \mathbf{A}_i, \mathbf{A}_j \in \mathbf{A}, -1 \leq |\mathbf{A}_i| - |\mathbf{A}_j| \leq 1$ 

1 begin
2    $baseCardinality \leftarrow \lfloor \frac{|\mathbf{n}|}{nAbs} \rfloor$ 
3    $extras \leftarrow |\mathbf{n}| \bmod nAbs$ 
4    $\mathbf{n}^* \leftarrow SORT(\mathbf{n}, \mu, \text{low-to-high})$ 
5    $j_{begin} \leftarrow 1$ 
6   foreach  $i \leftarrow 1, \dots, nAbs$  do
7     if  $extras > 0$  then
8        $j_{end} \leftarrow j_{begin} + baseCardinality$ 
9        $extras \leftarrow extras - 1$ 
10      else
11         $j_{end} \leftarrow j_{begin} + baseCardinality - 1$ 
12         $\mathbf{A}_i \leftarrow \{n_{j_{begin}}^*, \dots, n_{j_{end}}^*\}$ 
13         $j_{begin} \leftarrow j_{end} + 1$ 
14      end
15       $\mathbf{A} \leftarrow \cup_{i=1}^{nAbs} \mathbf{A}_i$ 
16      return  $\mathbf{A}$ 
17 end

```

The simpleVB (simple value-based) scheme follows the motivation of grouping nodes of similar value in the same abstract state by a simple 2-step method: 1) first, nodes are ordered by their heuristic value (low to high), and 2) next the ordered nodes are partitioned into [approximately] equal cardinality abstract states.

Time Complexity.

Partitioning is achieved via one pass through $|\mathbf{n}^*|$ leading to $\mathcal{O}(|\mathbf{n}| \log |\mathbf{n}|)$ time complexity due to sorting.

Space Complexity.

No more than linear space is required. $\mathcal{O}(|\mathbf{n}|)$

Result on Running Example.

$\{1.0, 1.1\}, \{1.2, 1.3\}, \{1.4, 1.5\}, \{10, 100\}$

Through its simplicity, this method aims to leverage speed allowing for abstractions to be formed much quicker leading to greater number of samples.

¹Such that nodes maintain sort order o across all abstract states.

6.0.2 minVarVB

$\Psi = \Psi_{minVarVB}$ (Algorithm 4)

Algorithm 4: $\Psi_{minVarVB}$

input : A set of nodes n to be partitioned into $nAbs$ abstract states; a value function $\mu(\cdot)$
output : n partitioned into abstract states¹ $A = \{A_i \mid i \in \{1, \dots, nAbs\}\}$ satisfying $\min \sum_{A_i \in A} Var(A_i, v)$

```

1 begin
2   | A = WardsMethod(n, nAbs, mu(.), Euclidian distance)
3   | return A
4 end

```

As mentioned in Section 4.2, Proposition 4.2.0.3, Rizzo [2007] showed that in stratified importance sampling minimizing variance of the estimates within individual strata can lead to a reduction in overall variance.

The minVarVB scheme was designed based on this intuition. The scheme uses Ward's Minimum Variance Hierarchical Clustering (or Ward's Method, for short) Ward [1963] to group nodes into a $nAbs$ abstract states so as to minimize variance within each abstract state with respect to the provided value function $\mu(\cdot)$.

Ward's Minimum Variance Hierarchical Clustering is an agglomerative hierarchical clustering algorithm designed to create a dendrogram by iteratively merging clusters. The primary objective is to minimize the total within-cluster variance. Ward's method works as outlined in Algorithm 5.

Algorithm 5: Ward's Method

1. **Initialization:** Treat each data point as an individual cluster. Assign each cluster a label or identifier.
 2. **Compute Pairwise Distances:** Calculate the pairwise distances between all clusters. Various distance metrics can be used, such as Euclidean distance.
 3. **Cluster Merging Iteration:**
 - (a) Identify the pair of clusters C_i and C_j that, when merged into a new cluster C_{ij} , results in the smallest increase in the overall within-cluster variance. This is determined using the formula:
$$\Delta Var = Var(C_{ij}) - (Var(C_i) + Var(C_j))$$
where $Var(C_{ij})$ is the variance of the merged cluster, and $Var(C_i)$ and $Var(C_j)$ are the variances of clusters C_i and C_j , respectively.
 - (b) Update distance measures between the newly merged cluster and all other clusters.
 4. **Repeat:** Repeat steps 2-3 until the desired number of clusters is achieved.
-

Ward's Method can be combined with Lance-Williams linear distance updates Lance and Williams [1967] to increase efficiency. Lance-Williams linear distance updates, in the context of agglomerative clustering, refer to the formula used to calculate the distance between clusters as they are merged during the hierarchical clustering process. The general form of Lance-Williams distance updates can be expressed as follows:

$$d_{(ij)k} = \alpha_i d_{ik} + \alpha_j d_{jk} + \alpha d_{ij} + \gamma |d_{ik} - d_{jk}| \quad (5)$$

where:

- d_{ij} , d_{ik} , and d_{jk} are the pair-wise distances between clusters C_i , C_j , and C_k
- $d_{(ij)k}$ is the distance between the newly merged cluster $C_i \cup C_j$ and cluster C_k
- α_i , α_j , α , and γ are coefficients that depend on the linkage criterion used

In the case of Ward's method, the coefficients are specific to the minimization of within-cluster variance and are calculated

as follows:

$$\begin{aligned}
 \alpha_i &= \frac{|C_i| + |C_k|}{|C_i| + |C_j| + |C_k|} \\
 \alpha_j &= \frac{|C_j| + |C_k|}{|C_i| + |C_j| + |C_k|} \\
 \alpha &= -\frac{|C_k|}{|C_i| + |C_j| + |C_k|} \\
 \gamma &= 0
 \end{aligned} \tag{6}$$

(The inclusion of γ provides additional flexibility in the more general case, adjusting the distance updates based on the specific clustering criterion being used).

Time Complexity.²

The choice of clusters to merge generally leads to having a $\mathcal{O}(|n|^3)$ time complexity due to the need to compare pair-wise distances between all clusters at each iteration. However, in the case where nodes are distributed linearly in one dimension, use of a priority queue, and using Lance-Williams distance updates, the time complexity is can be reduced to $\mathcal{O}(|n|^2)$.

Space Complexity.²

The space complexity is implementation dependent, with most time-efficient variants making use of a distance matrix leading to $\mathcal{O}(|n|^2)$ space complexity.

Result on Running Example.

$\{1.0, 1.1, 1.2\}, \{1.3, 1.4, 1.5\}, \{10\}, \{100\}$

In contrast to simpleVB, minVarVB places considerable resources into computing abstractions, leading to fewer samples, but with potentially better estimates with an appropriate value function $\mu(\cdot)$.

6.0.3 equalDistVB

$\Psi_{equalDistVB}$ (Algorithm 6)

Algorithm 6: $\Psi_{equalDistVB}$

input : A set of nodes n to be partitioned into $nAbs$ abstract states; a value function $\mu(\cdot)$
output : With $\mu(A_1, \dots, i) = (\sum_{j=1}^i \sum_{n' \in A_j} \mu(n'), n_{A_i}^{last}$ be the last node in A_i , and $\mathcal{Q}_i = \frac{i \cdot \sum_{n \in n^*} \mu(n)}{nAbs}$, n partitioned into abstract states¹ $A = \{A_i \mid i \in \{1, \dots, nAbs\}\}$ such that for $i = 1, \dots, nAbs$ in order, ($\mu(A_1, \dots, i) \geq \mathcal{Q}_i$) \wedge ($(A_i = \{\}) \vee (\mu(A_1, \dots, i) - \mu(n_{A_i}^{last}) < \mathcal{Q}_i)$)

```

1 begin
2    $n^* \leftarrow SORT(n, \mu, \text{low-to-high})$ 
3    $j \leftarrow 1$ 
4   foreach  $i \leftarrow 1, \dots, nAbs$  do
5      $A_i \leftarrow \{\}$ 
6     while  $\mu(A_1, \dots, i) < \mathcal{Q}_i$  do
7        $A_i \leftarrow A_i \cup \{n_j^*\}$ 
8        $j \leftarrow j + 1$ 
9     end
10   end
11    $A \leftarrow \bigcup_{i=1}^{nAbs} A_i$ 
12   return  $A$ 
13 end

```

In sampling it is generally beneficial to predominantly sample high impact regions of the search/sampling space. Allowing the provided value function $\mu(\cdot)$ to serve as a heuristic of nodes that are part of these high impact spaces, equalDistVB attempts to balance this intuition with the notion of variance reduction from minVarVB in attempts to group fewer predicted high impact nodes together in abstract states and allowing for the predicted lower impact nodes to be part of larger abstract states. Also inspired by the simplicity of simpleVB, the scheme works by greedily adding nodes in value order (low to high) into abstract state A_i until the total sum of node values from A_1, \dots, A_i reaches or exceeds the $\frac{i}{nAbs}$ quantile.

²Assuming $\mu(n)$ is $\mathcal{O}(1)$ in both time and space.

When paired with the QB abstraction class, the equalDistVB schemes also attempts to partition notes into abstract states of equal mass under the proposal. This corresponds to the condition for Proposition 4.2.0.3 for stratified importance sampling variance reduction.

Time Complexity.²

$\mu(\mathbf{A}_{1\dots i})$ can be updated progressively in constant time, and thus computation of \mathcal{Q}_i at each iteration can also be done in constant time. Partitioning is achieved via one pass through $|\mathbf{n}^*|$ leading to $\mathcal{O}(|\mathbf{n}| \log |\mathbf{n}|)$ time complexity due to sorting.

Space Complexity.²

No more than linear space is required. $\mathcal{O}(|\mathbf{n}|)$

Result on Running Example.

$\{1.0, 1.1, 1.2, 1.3, 1.4, 1.5, 10, 100\}, \{\}, \{\}, \{\}$

Although, this method hopes to find a balance between intuitions previously explored, and without compromising speed and efficiency of abstract state generation, from the running example we can see how this method yield undesirable results in the presence of certain distributions of node values. In this example, the first quantile is only reached after all the nodes have been added to the first abstract state, leaving no nodes remaining to be partitioned into the subsequent abstract states.

6.0.4 equalDistVB2

$\Psi_{equalDistVB2}$ (Algorithm 7)

Algorithm 7: $\Psi_{equalDistVB2}$

input : A set of nodes \mathbf{n} to be partitioned into $nAbs$ abstract states; a value function $\mu(\cdot)$
output : With $\mu(\mathbf{A}_{1\dots i}) = (\sum_{j=1}^i \sum_{n' \in \mathbf{A}_j} \mu(n'), n_{\mathbf{A}_i}^{last}$ be the last node in \mathbf{A}_i , and $\mathcal{Q}_i = \frac{i \cdot \sum_{n \in \mathbf{n}^*} \mu(n)}{nAbs}$, \mathbf{n} partitioned into abstract states¹ $\mathbf{A} = \{\mathbf{A}_i \mid i \in \{1, \dots, nAbs\}\}$ such that for $i = 1, \dots, nAbs$ in order, ($\mu(\mathbf{A}_{1\dots i}) \geq \mathcal{Q}_i$) \wedge ($(\mathbf{A}_i = \{\}) \vee (\mu(\mathbf{A}_{1\dots i}) - \mu(n_{\mathbf{A}_i}^{last}) < \mathcal{Q}_i)$)

```

1 begin
2    $\mathbf{n}^* \leftarrow SORT(\mathbf{n}, \mu, \text{high-to-low})$ 
3    $j \leftarrow 1$ 
4   foreach  $i \leftarrow 1, \dots, nAbs$  do
5      $\mathbf{A}_i \leftarrow \{\}$ 
6     while  $\mu(\mathbf{A}_{1\dots i}) < \mathcal{Q}_i$  do
7        $\mathbf{A}_i \leftarrow \mathbf{A}_i \cup \{n_j^*\}$ 
8        $j \leftarrow j + 1$ 
9     end
10   end
11    $\mathbf{A} \leftarrow \bigcup_{i=1}^{nAbs} \mathbf{A}_i$ 
12   return  $\mathbf{A}$ 
13 end

```

By simply reversing the sort order, equalDistVB2 is able to use the same partitioning strategy $\Psi_{equalDistVB}$ associated with equalDistVB meanwhile mitigate some of the overfilling of abstract states.

Time Complexity.²

$\mu(\mathbf{A}_{1\dots i})$ can be updated progressively in constant time, and thus computation of \mathcal{Q}_i at each iteration can also be done in constant time. Partitioning is achieved via one pass through $|\mathbf{n}^*|$ leading to $\mathcal{O}(|\mathbf{n}| \log |\mathbf{n}|)$ time complexity due to sorting.

Space Complexity.²

No more than linear space is required. $\mathcal{O}(|\mathbf{n}|)$

Result on Running Example.

$\{100\}, \{\}, \{\}, \{10, 1.5, 1.4, 1.3, 1.2, 1.1, 1.0\}$

We see that equalDistVB2 can still be subject to over packing of abstract states. Next we present two more equalDistVB variants that continue to mitigate this artifact.

6.0.5 equalDistVB3

$\Psi_{equalDistVB3}$ (Algorithm 8)

Algorithm 8: $\Psi_{equalDistVB3}$

input : A set of nodes n to be partitioned into $nAbs$ abstract states; a value function $\mu(\cdot)$
output : With $\mu(A_{1,\dots,i}) = (\sum_{j=1}^i \sum_{n' \in A_j} \mu(n'), n_{A_i}^{last}$ be the last node in A_i , and $\mathcal{Q}_i = \frac{i \cdot \sum_{n \in n^*} \mu(n)}{nAbs}$, n partitioned into
abstract states¹ $A = \{A_i \mid i \in \{1, \dots, nAbs\}\}$ such that for $i = 1, \dots, nAbs$ in order, ($\mu(A_{1,\dots,i}) \geq \mathcal{Q}_i$) \wedge
($|A_i| = 1$) \vee ($\mu(A_{1,\dots,i}) - \mu(n_{A_i}^{last}) < \mathcal{Q}_i$)

```

1 begin
2    $n^* \leftarrow SORT(n, \mu, \text{high-to-low})$ 
3    $j \leftarrow 1$ 
4   foreach  $i \leftarrow 1, \dots, nAbs$  do
5      $A_i \leftarrow \{n_j^*\}$ 
6      $j \leftarrow j + 1;$ 
7     while  $\mu(A_{1,\dots,i}) < \mathcal{Q}_i$  do
8        $A_i \leftarrow A_i \cup \{n_j^*\}$ 
9        $j \leftarrow j + 1$ 
10    end
11  end
12   $A \leftarrow \cup_{i=1}^{nAbs} A_i$ 
13  return  $A$ 
14 end
```

In order to lessen over packing and ensure abstract states are not left empty, equalDistVB3 modifies equalDistVB2 so that, after processing of each abstract state, the next state is forced an addition of at least a single node by default.

Time Complexity.²

$\mu(A_{1\dots i})$ can be updated progressively in constant time, and thus computation of \mathcal{Q}_i at each iteration can also be done in constant time. Partitioning is achieved via one pass through $|n^*|$ leading to $\mathcal{O}(|n| \log |n|)$ time complexity due to sorting.

Space Complexity.²

No more than linear space is required. $\mathcal{O}(|n|)$

Result on Running Example.

{100}, {10}, {1.5}, {1.4, 1.3, 1.2, 1.1, 1.0}

Still highly efficient, equalDistVB3 manages to ensure that the provided $nAbs$ granularity is honored, allowing users better control of the search vs. sampling interpolation possible with Abstraction Sampling.

6.0.6 equalDistVB4

$\Psi_{equalDistVB4}$ (Algorithm 9)

The final variant of the equalDist schemes, equalDistVB4 attempts to perform a more even partitioning than the previous variants by recomputing quantiles. Each time the algorithm progresses to processing a new abstract state, remaining nodes and abstract states are used to compute new quantiles which are then used to guide filling of the current abstract state in the same way previously done.

Time Complexity.²

$\mu(A_{1\dots i})$ can be updated progressively in constant time, and thus computation of $\widehat{\mathcal{Q}}_i$ at each iteration can also be done in constant time. Partitioning is achieved via one pass through $|n^*|$ leading to $\mathcal{O}(|n| \log |n|)$ time complexity due to sorting.

Space Complexity.²

No more than linear space is required. $\mathcal{O}(|n|)$

Result on Running Example.

{100}, {10}, {1.5, 1.4, 1.3}, {1.2, 1.1, 1.0}

Still highly efficient, equalDistVB3 manages to ensure that the provided $nAbs$ granularity is honored, allowing users better

Algorithm 9: $\Psi_{equalDistVB4}$

input : A set of nodes n to be partitioned into $nAbs$ abstract states; a value function $\mu(\cdot)$
output : With $\mu(A_1, \dots, i) = (\sum_{j=1}^i \sum_{n' \in A_j} \mu(n'), n_{A_i}^{\text{last}}$ be the last node in A_i , and $\hat{Q}_i = \frac{\mu(n^*) - \mu(A_1, \dots, i-1)}{nAbs-i+1}$, n partitioned
 into abstract states¹ $A = \{A_i \mid i \in \{1, \dots, nAbs\}\}$ such that for $i = 1, \dots, nAbs$ in order, ($\mu(A_i) \geq \hat{Q}_i$) \wedge
 ($(|A_i| = 1) \vee (\mu(A_i) - \mu(n_{A_i}^{\text{last}}) < \hat{Q}_i)$)

```

1 begin
2    $n^* \leftarrow SORT(n, \mu, \text{high-to-low})$ 
3    $j \leftarrow 1$ 
4   foreach  $i \leftarrow 1, \dots, nAbs$  do
5      $A_i \leftarrow \{\}$ 
6     while  $\mu(A_i) < \hat{Q}_i$  do
7        $A_i \leftarrow A_i \cup \{n_j^*\}$ 
8        $j \leftarrow j + 1$ 
9     end
10   end
11    $A \leftarrow \cup_{i=1}^{nAbs} A_i$ 
12   return  $A$ 
13 end
```

control of the search vs. sampling interpolation possible with Abstraction Sampling.

6.0.7 randVB

Ψ_{randVB} (Algorithm 10)

Algorithm 10: Ψ_{randVB}

input : A set of nodes n to be partitioned into $nAbs$ abstract states; a value function $\mu(\cdot)$
output : n partitioned into abstract states¹ $A = \{A_i \mid i \in \{1, \dots, nAbs\}\}$

```

1 begin
2    $n^* \leftarrow SORT(n, \mu, \text{high-to-low})$ 
3    $s \sim Unif(\{M \subseteq \{1, \dots, |n^*| - 1\} \mid |M| = nAbs - 1\})$ 
4    $s^* \leftarrow SORT(s)$ 
5    $j \leftarrow 1$ 
6   foreach  $i \leftarrow 1, \dots, nAbs - 1$  do
7      $A_i = \{n_j^*, \dots, n_{s_i^*}^*\}$ 
8      $j \leftarrow s_i^* + 1$ 
9   end
10   $A_{nAbs} = \{n_j^*, \dots, n_{|n^*|}^*\}$ 
11   $A = \cup_{i=1}^{nAbs} A_i$ 
12  return  $A$ 
13 end
```

If the quality of $\mu(\cdot)$ as a measure of similarity is unknown or poor, it could instead be beneficial to rely on randomness to ensure a diverse sampling of abstractions. randVB does this by sampling $nAbs - 1$ partition points between the sorted nodes n^* uniformly at random and without replacement, and then partitions the nodes accordingly. As a result, abstract states are formed such that nodes are still grouped according to $\mu(\cdot)$, but the size of those groups varies.

Time Complexity.²

$\mathcal{O}(|n| \log |n|)$ time complexity due to sorting.

Space Complexity.²

No more than linear space is required. $\mathcal{O}(|n|)$

Result on Running Example.

$\{100, 10\}, \{1.5\}, \{1.4, 1.3, 1.2\}, \{1.1, 1.0\};$
 $\{100\}, \{10, 1.5, 1.4, 1.3\}, \{1.2, 1.1\}, \{1.0\}; \dots$ etc.

7 EXTENDED RESULTS

In extension to the main paper, here we show a more comprehensive set of aggregated data tables, now also including the standard deviation of the errors, the average number of samples drawn, and average probe sizes.

7.1 SUMMARY COMPARISON.

7.1.1 Exact Problems

iB-5, t-1300sec, Exact			DBN				
Class	Scheme	nAbs	Fail	Avg. Error	std(Avg. Error)	Avg. Num. Samples	Avg. Probe Size
HB	simple	2048	0	0.440	0.862	354	233936
	minVar	1	0	1.361	2.840	600260	136
	equalDist	1	0	1.365	2.835	634640	136
	equalDist2	1	0	1.570	3.292	493719	196
	equalDist3	1	0	1.489	3.018	489934	196
	equalDist4	1024	0	2.819	5.501	114	2965761
HRB	rand	256	0	0.496	0.796	2840	30952
	simple	2048	0	0.491	0.976	353	233936
	minVar	1	0	1.500	2.972	635538	136
	equalDist	1	0	1.305	2.508	654598	136
	equalDist2	1	0	1.549	3.405	664595	136
	equalDist3	1	0	1.405	3.014	662702	136
QB	equalDist4	1	0	1.511	3.064	664347	136
	rand	2048	0	0.451	0.719	358	233936
	simple	1	0	1.469	2.920	677854	136
	minVar	2048	0	0.050	0.173	10	233936
	equalDist	4	0	1.174	2.407	478845	181
	equalDist2	2048	0	0.736	1.831	17787	3326
CTX	equalDist3	2048	0	0.042	0.137	346	233936
	equalDist4	2048	0	0.130	0.378	1969	153490
	rand	1	0	1.295	2.723	683431	136
	rel	1	0	1.381	2.626	197143	476
	rand	4	0	1.472	3.093	695636	136
RAND	rand	2048	0	0.104	0.243	359	233936

Table 1

iB-5, t-300sec, Exact			Grids				
Class	Scheme	nAbs	Fail	Avg. Error	std(Avg. Error)	Avg. Num. Samples	Avg. Probe Size
HB	simple	1024	0	2.202	3.807	1536	365339
	minVar	16	0	3.251	5.615	37401	6295
	equalDist	2048	0	10.854	19.810	12787	36088
	equalDist2	512	0	8.050	14.709	44538	11654
	equalDist3	2048	0	2.764	4.210	588	805429
	equalDist4	64	0	6.029	11.585	10521	359937
HRB	rand	2048	0	2.248	3.933	709	737966
	simple	4	0	9.667	17.275	441504	1678
	minVar	64	0	2.319	3.816	3046	25570
	equalDist	256	0	10.635	18.892	86568	6357
	equalDist2	2048	0	6.790	11.752	12056	35124
	equalDist3	1024	0	2.292	3.951	1259	396048
QB	equalDist4	512	0	1.829	3.057	2787	188320
	rand	4	0	6.122	10.479	465813	1643
	simple	16	0	10.076	17.905	113719	6499
	minVar	1024	0	1.566	2.844	14	397296
	equalDist	2048	0	8.134	16.643	12162	70457
	equalDist2	2048	0	4.405	9.051	11932	71415
CTX	equalDist3	2048	0	1.771	3.391	612	788719
	equalDist4	512	0	1.754	3.159	2793	190568
	rand	256	0	6.048	10.294	6041	100691
	rel	64	0	5.030	9.168	471163	1421
	rand	4	0	4.021	7.528	36934	14867
RAND	rand	1024	0	1.501	2.530	1504	390548

Table 2

iB-5, t-300sec, Exact			Pedigree				
Class	Scheme	nAbs	Fail	Avg. Error	std(Avg. Error)	Avg. Num. Samples	Avg. Probe Size
HB	simple	2048	0	0.150	0.564	393	1208067
	minVar	64	0	0.422	0.894	1904	34760
	equalDist	1024	0	0.303	0.626	1104	406884
	equalDist2	1024	0	0.315	0.536	1090	410306
	equalDist3	1024	0	0.279	0.539	727	606552
	equalDist4	512	0	0.214	0.622	1526	305759
	rand	2048	0	0.185	0.473	406	1170793
HRB	simple	256	0	0.225	0.378	3637	155656
	minVar	256	0	0.309	0.543	131	149534
	equalDist	1024	0	0.638	0.921	1653	247759
	equalDist2	16	0	0.457	0.646	83869	5396
	equalDist3	16	0	0.537	0.843	63832	8067
	equalDist4	64	0	0.483	0.836	14789	34813
	rand	64	0	0.666	0.983	17216	36226
QB	simple	256	0	0.297	0.510	3672	153687
	minVar	64	0	0.210	0.561	1939	36977
	equalDist	2048	0	0.144	0.646	524	808760
	equalDist2	1024	0	0.145	0.637	1067	410631
	equalDist3	512	0	0.148	0.643	1403	324983
	equalDist4	512	0	0.134	0.600	1415	322792
	rand	16	0	0.740	1.021	76974	8055
CTX	rand	16	0	0.540	0.827	169911	2790
	rel	64	0	0.424	0.653	28214	29061
RAND	rand	1024	0	0.143	0.619	878	620063

Table 3

iB-5, t-300sec, Exact			Promedas				
Class	Scheme	nAbs	Fail	Avg. Error	std(Avg. Error)	Avg. Num. Samples	Avg. Probe Size
HB	simple	1024	0	0.575	1.288	7878163	215898
	minVar	16	2	2.509	5.329	4119191	2304
	equalDist	1024	0	2.332	3.857	8057221	145513
	equalDist2	64	0	2.123	4.632	8086745	8209
	equalDist3	256	0	2.196	4.354	8212578	53287
	equalDist4	2048	0	1.355	2.486	8106429	471471
	rand	2048	0	0.752	1.476	8136226	382946
HRB	simple	2048	0	0.705	1.594	8281435	444640
	minVar	16	1	2.801	5.552	8302630	2403
	equalDist	16	4	4.055	7.212	8505442	1255
	equalDist2	16	2	3.445	6.549	8445561	1667
	equalDist3	16	2	2.656	5.561	8389700	2330
	equalDist4	2048	0	2.024	3.247	8278922	429451
	rand	1024	1	2.165	4.691	8284836	184056
QB	simple	256	1	3.164	5.634	8156519	44804
	minVar	64	1	1.062	3.999	8149950	13097
	equalDist	2048	0	0.583	1.053	8159447	85975
	equalDist2	2048	0	0.539	1.098	8146812	87006
	equalDist3	2048	0	0.412	0.917	8136397	517395
	equalDist4	512	0	0.437	1.062	8155880	126503
	rand	16	2	5.988	12.148	8401169	1892
CTX	rand	1024	1	2.442	4.755	8045093	2016
	rel	64	6	4.349	7.852	8384108	3268
RAND	rand	1024	0	0.513	1.033	8047804	228960

Table 4

7.1.2 LARGE Problems

iB-10, t-1200sec, LARGE			DBN				
Class	Scheme	nAbs	Fail	Avg. Error	std(Avg. Error)	Avg. Num. Samples	Avg. Probe Size
HB	simple	512	0	3.059	5.994	466	213236
	minVar	1	0	6.372	10.410	170425	434
	equalDist	1	0	6.354	10.259	171742	434
	equalDist2	1	0	6.172	9.889	146566	598
	equalDist3	1	0	6.548	10.206	144646	598
	equalDist4	1	0	6.525	10.576	162296	434
	rand	64	0	1.855	2.986	3682	27039
HRB	simple	2048	0	3.202	6.388	116	844724
	minVar	1	0	6.102	9.811	167382	434
	equalDist	1	0	6.273	10.219	165303	434
	equalDist2	1	0	6.689	10.719	164615	434
	equalDist3	1	0	6.564	10.301	163186	434
	equalDist4	1	0	6.606	10.704	162441	434
	rand	2048	0	1.915	3.994	116	844724
QB	simple	1	0	6.540	10.583	162844	434
	minVar	2048	0	1.837	4.023	11	844724
	equalDist	512	0	5.423	9.545	28518	50129
	equalDist2	2048	0	3.813	7.105	11104	162286
	equalDist3	2048	0	1.645	3.853	115	844724
	equalDist4	2048	0	1.643	3.847	170	758313
	rand	4	0	6.292	9.781	52602	1721
CTX	rand	64	0	5.710	8.760	4947	22519
	rel	1	0	6.267	10.128	165870	434
RAND	rand	2048	0	2.123	4.214	116	844724

Table 5

iB-10, t-1200sec, LARGE			Grids				
Class	Scheme	nAbs	Fail	Avg. Error	std(Avg. Error)	Avg. Num. Samples	Avg. Probe Size
HB	simple	2048	0	73.710	117.967	585	5281698
	minVar	64	0	71.628	112.070	1948	184817
	equalDist	2048	0	149.888	252.503	6894	438547
	equalDist2	1024	0	119.823	195.442	12859	247710
	equalDist3	64	0	82.927	124.857	15758	197893
	equalDist4	1024	0	63.194	97.515	1020	2846847
	rand	2048	0	82.203	132.286	527	5492402
HRB	simple	1024	0	193.654	311.138	1042	3061184
	minVar	512	0	37.972	56.653	29	1534848
	equalDist	2048	0	127.990	216.992	6524	475696
	equalDist2	2048	0	104.502	168.754	6388	501514
	equalDist3	2048	0	38.936	52.976	429	6090687
	equalDist4	2048	0	34.676	50.051	460	5664129
	rand	16	0	160.168	262.678	78263	48729
QB	simple	16	0	197.931	331.349	73034	51032
	minVar	1024	0	28.423	44.701	7	3064517
	equalDist	2048	0	118.547	209.112	6013	932447
	equalDist2	2048	0	91.994	160.979	5935	939064
	equalDist3	2048	0	19.277	31.795	429	6135039
	equalDist4	2048	0	18.866	34.470	462	5658527
	rand	16	0	163.973	270.397	78137	48849
CTX	rand	512	0	111.104	189.309	53385	66495
	rel	1024	0	80.633	131.304	1990	1210381
RAND	rand	2048	0	19.053	30.561	517	5915471

Table 6

Linkage-Type4							
			Fail	Avg. Error	std(Avg. Error)	Avg. Num. Samples	Avg. Probe Size
HB	simple	2048	21	47.383	124.818	215	6362535
	minVar	256	37	133.377	208.955	118	526228
	equalDist	2048	37	136.462	209.952	806	1725651
	equalDist2	2048	36	132.531	206.716	775	1763041
	equalDist3	2048	32	118.653	191.472	373	4231305
	equalDist4	2048	29	98.222	180.908	260	5348049
	rand	2048	21	52.171	117.178	258	5548243
HRB	simple	2048	17	48.474	105.528	201	7170175
	minVar	512	38	138.131	211.272	31	1203151
	equalDist	2048	32	123.253	192.089	1138	1438777
	equalDist2	2048	34	129.751	198.056	1114	1453506
	equalDist3	2048	31	118.091	185.967	405	4586845
	equalDist4	2048	26	95.895	158.305	335	5182785
	rand	1024	18	127.021	162.172	576	3170049
QB	simple	2048	13	48.681	102.256	165	7582217
	minVar	256	31	93.058	176.650	115	595380
	equalDist	2048	22	46.196	128.408	324	3606296
	equalDist2	1024	21	40.310	115.108	823	1613744
	equalDist3	1024	20	37.490	115.666	428	3151667
	equalDist4	2048	16	30.512	104.300	155	7276760
	rand	256	17	156.992	197.622	2123	786014
CTX	rand	2048	53	194.741	250.879	78237	12693
	rel	1024	37	129.189	210.249	911	2128473
RAND	rand	1024	19	33.804	107.942	531	3043774

Table 7

Promedas							
			Fail	Avg. Error	std(Avg. Error)	Avg. Num. Samples	Avg. Probe Size
HB	simple	1024	16	5.981	14.402	5303	316842
	minVar	16	25	9.433	17.375	135360	3961
	equalDist	64	23	9.664	16.936	122333	11729
	equalDist2	16	22	9.465	17.026	438953	3209
	equalDist3	16	18	8.534	16.129	364644	3961
	equalDist4	16	19	8.011	15.663	368986	3973
	rand	64	22	8.296	16.348	129906	14836
HRB	simple	512	15	5.849	14.157	10763	158416
	minVar	16	24	9.577	17.048	130796	4001
	equalDist	16	32	11.596	19.010	546356	2629
	equalDist2	4	25	10.380	17.881	1755156	841
	equalDist3	16	22	9.779	17.253	388573	3844
	equalDist4	16	22	9.217	16.843	383539	3876
	rand	64	27	9.556	17.661	128420	15010
QB	simple	4	34	11.919	19.156	2214241	849
	minVar	16	13	5.403	13.076	127451	4261
	equalDist	512	15	5.960	13.509	21151	61005
	equalDist2	2048	12	4.982	12.955	5495	230190
	equalDist3	256	5	2.560	8.629	16078	90936
	equalDist4	512	5	2.476	8.229	7638	187975
	rand	4	28	11.532	19.413	2330332	841
CTX	rand	256	0	3.222	5.085	160087	12862
	rel	16	34	11.247	18.992	761684	2399
RAND	rand	1024	10	3.936	11.615	5010	348002

Table 8

7.2 COMPARISON USING 100 SAMPLES.

7.2.1 Exact Problems

Table 9

iB-5, m-100, Exact			DBN		Grids		Pedigree		Promedas	
Class	Scheme	nAbs	Fail	Avg. Error	Fail	Avg. Error	Fail	Avg. Error	Fail	Avg. Error
HB	simpleQB	256	0	1.601	0	4.768	0	0.337	14	3.121
	minVarQB	256	0	5.028	0	5.134	0	0.615	1	5.423
	equalDist	256	0	5.269	0	15.958	1	2.145	13	6.556
	equalDist2	256	0	5.966	0	11.009	0	1.384	6	6.464
	equalDist3	256	0	6.203	0	5.804	0	0.669	1	5.480
	equalDist4	256	0	4.501	0	22.576	0	1.103	1	4.382
HRB	randQB	256	0	0.712	0	5.515	0	0.531	13	4.988
	simpleQB	256	0	1.638	0	15.757	0	0.721	14	3.014
	minVarQB	256	0	4.703	0	2.404	0	0.287	1	4.295
	equalDist	256	0	6.030	0	16.132	1	2.817	13	8.830
	equalDist2	256	0	6.361	0	10.462	0	2.546	6	8.272
	equalDist3	256	0	6.613	0	4.236	0	2.291	1	7.427
QB	equalDist4	256	0	6.753	0	3.179	0	1.241	1	5.552
	randQB	256	0	0.720	0	9.838	0	1.818	13	7.074
	simpleQB	256	0	5.350	0	17.406	0	1.059	14	9.659
	minVarQB	256	0	0.111	0	1.911	0	0.223	1	1.634
	equalDist	256	0	5.619	0	15.533	1	0.858	13	5.420
	equalDist2	256	0	2.319	0	11.220	0	0.563	6	3.479
CTX	equalDist3	256	0	0.173	0	3.615	0	0.206	1	1.473
	equalDist4	256	0	0.277	0	2.305	0	0.180	1	1.373
	randQB	256	0	4.982	0	12.653	0	3.211	13	19.441
	rand	256	0	3.587	0	9.568	2	4.695	3	14.386
	rel	256	0	5.265	0	8.013	0	1.097	36	10.845
RAND	rand	256	0	0.288	0	2.464	0	0.325	3	2.570

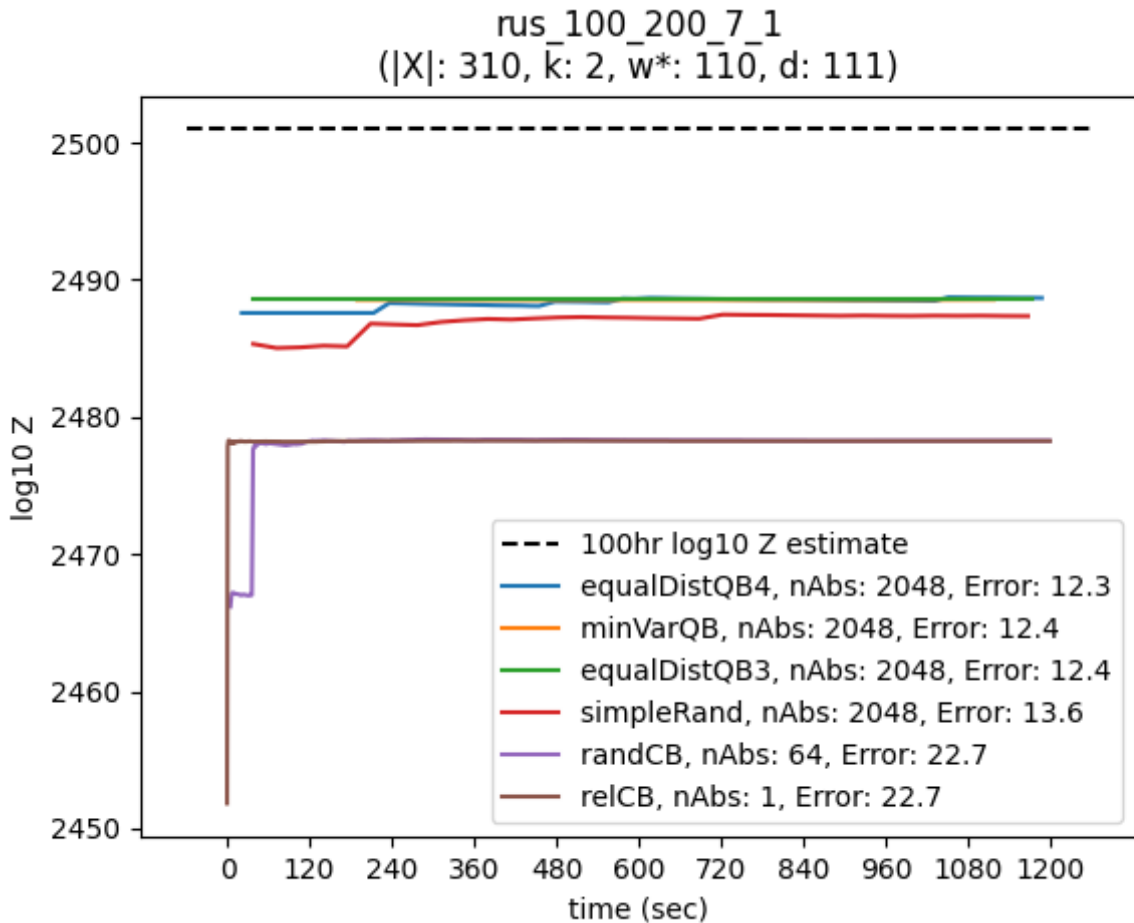
7.2.2 LARGE Problems

Table 10

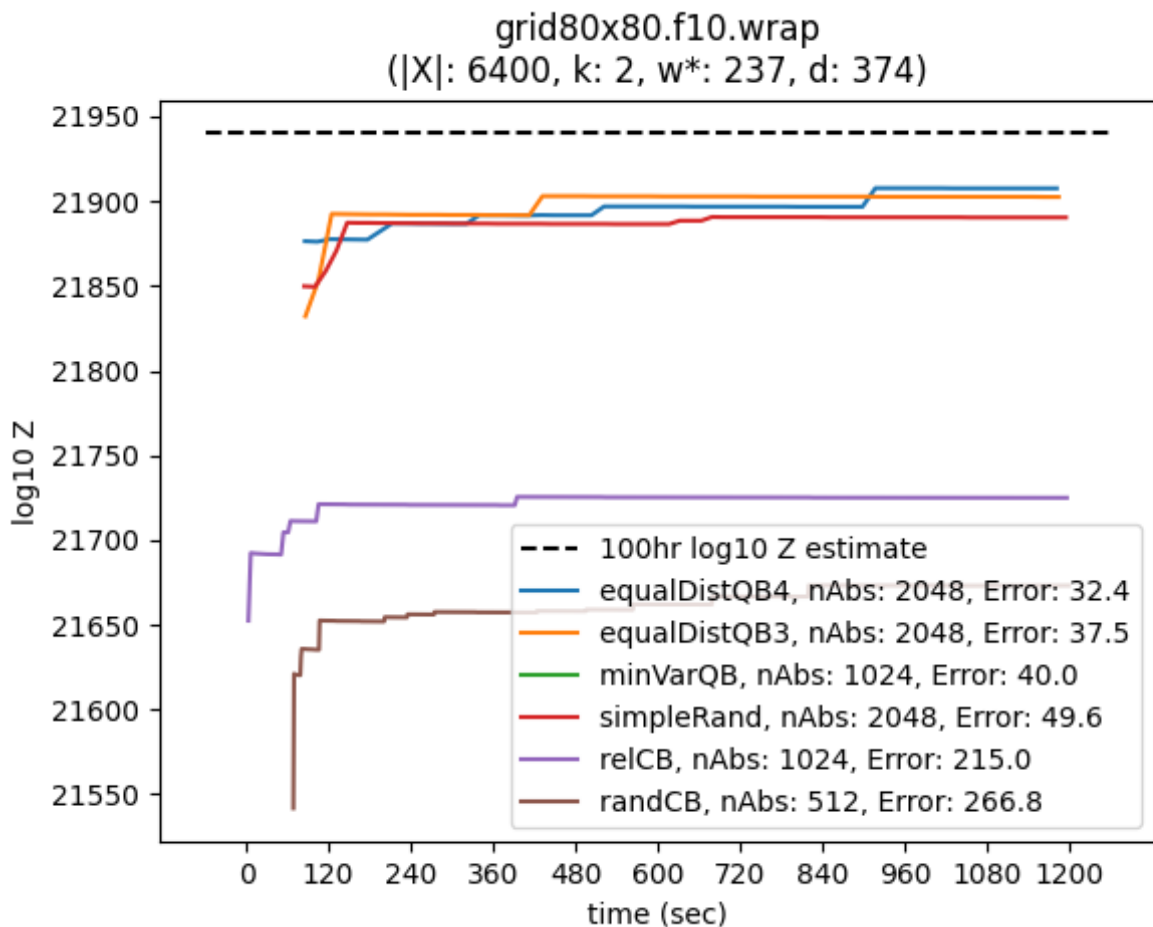
iB-10, m-100, LARGE			DBN		Grids		Linkage-Type4		Promedas	
Class	Scheme	nAbs	Fail	Avg. Error	Fail	Avg. Error	Fail	Avg. Error	Fail	Avg. Error
HB	simpleQB	256	0	4.179	0	108.953	0	189.141	14	16.389
	minVarQB	256	0	8.219	0	45.460	0	182.791	1	17.221
	equalDist	256	0	8.013	0	164.767	1	230.627	13	19.890
	equalDist2	256	0	8.233	0	119.203	0	231.620	6	18.944
	equalDist3	256	0	7.905	0	67.626	0	219.364	1	18.612
	equalDist4	256	0	7.588	0	54.643	0	199.565	1	17.186
HRB	randQB	256	0	3.741	0	108.760	0	203.436	13	18.494
	simpleQB	256	0	4.203	0	190.126	0	180.424	14	15.857
	minVarQB	256	0	7.770	0	29.575	0	188.654	1	17.492
	equalDist	256	0	7.947	0	151.765	1	235.331	13	20.390
	equalDist2	256	0	8.616	0	114.215	0	229.609	6	20.395
	equalDist3	256	0	7.653	0	37.005	0	222.866	1	19.932
QB	equalDist4	256	0	8.201	0	31.368	0	213.918	1	18.694
	randQB	256	0	3.254	0	150.130	0	205.219	13	19.157
	simpleQB	256	0	7.921	0	194.220	0	180.487	14	22.732
	minVarQB	256	0	2.848	0	22.838	0	182.296	1	11.742
	equalDist	256	0	6.443	0	140.283	1	192.449	13	17.245
	equalDist2	256	0	4.583	0	96.859	0	193.109	6	15.704
CTX	equalDist3	256	0	3.036	0	25.042	0	170.706	1	11.426
	equalDist4	256	0	2.715	0	20.978	0	162.793	1	11.885
	randQB	256	0	7.791	0	163.214	0	205.186	13	23.984
	rand	256	0	4.789	0	97.951	2	232.778	3	16.285
	rel	256	0	7.664	0	65.146	0	188.194	36	20.609
RAND	rand	256	0	3.070	0	26.185	0	178.273	3	13.957

7.3 TIME SERIES PLOT

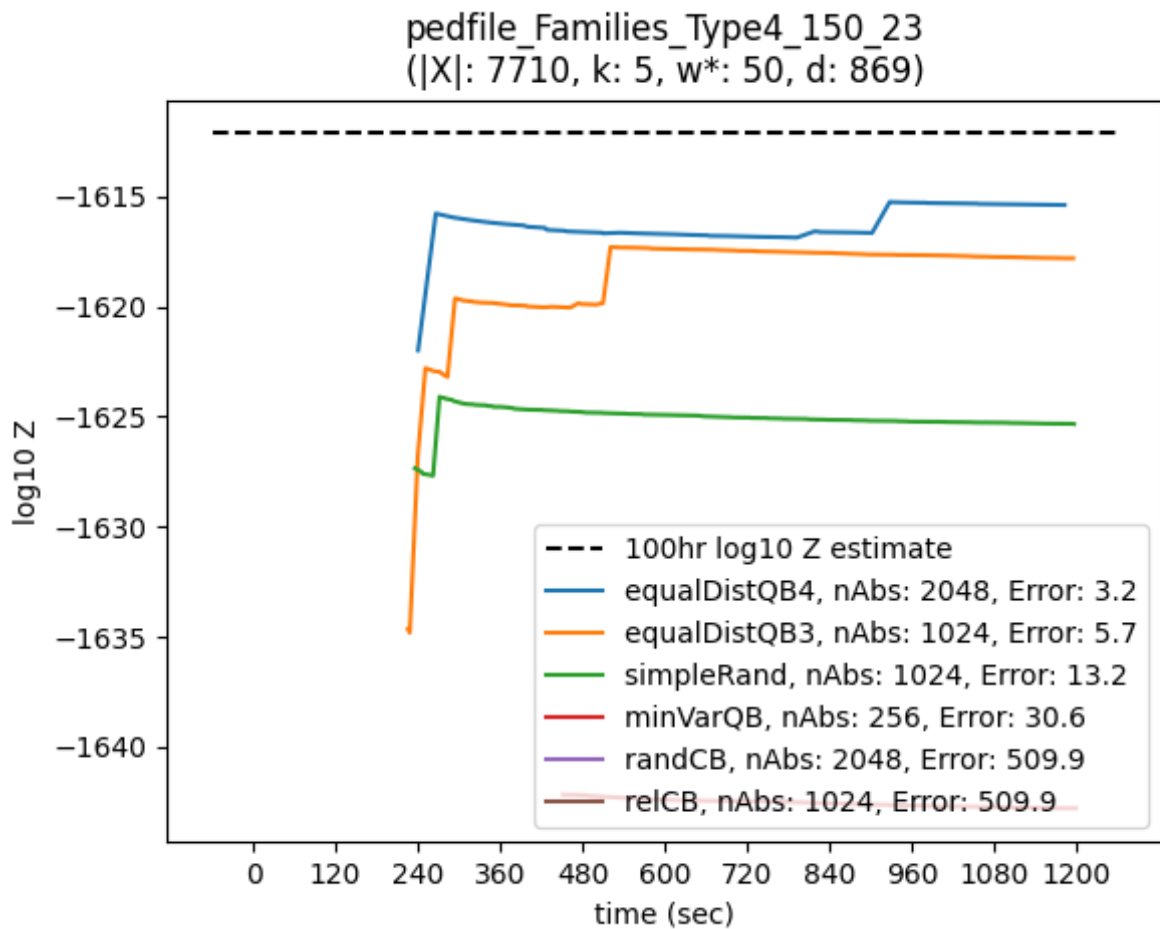
7.3.1 LARGE Problems



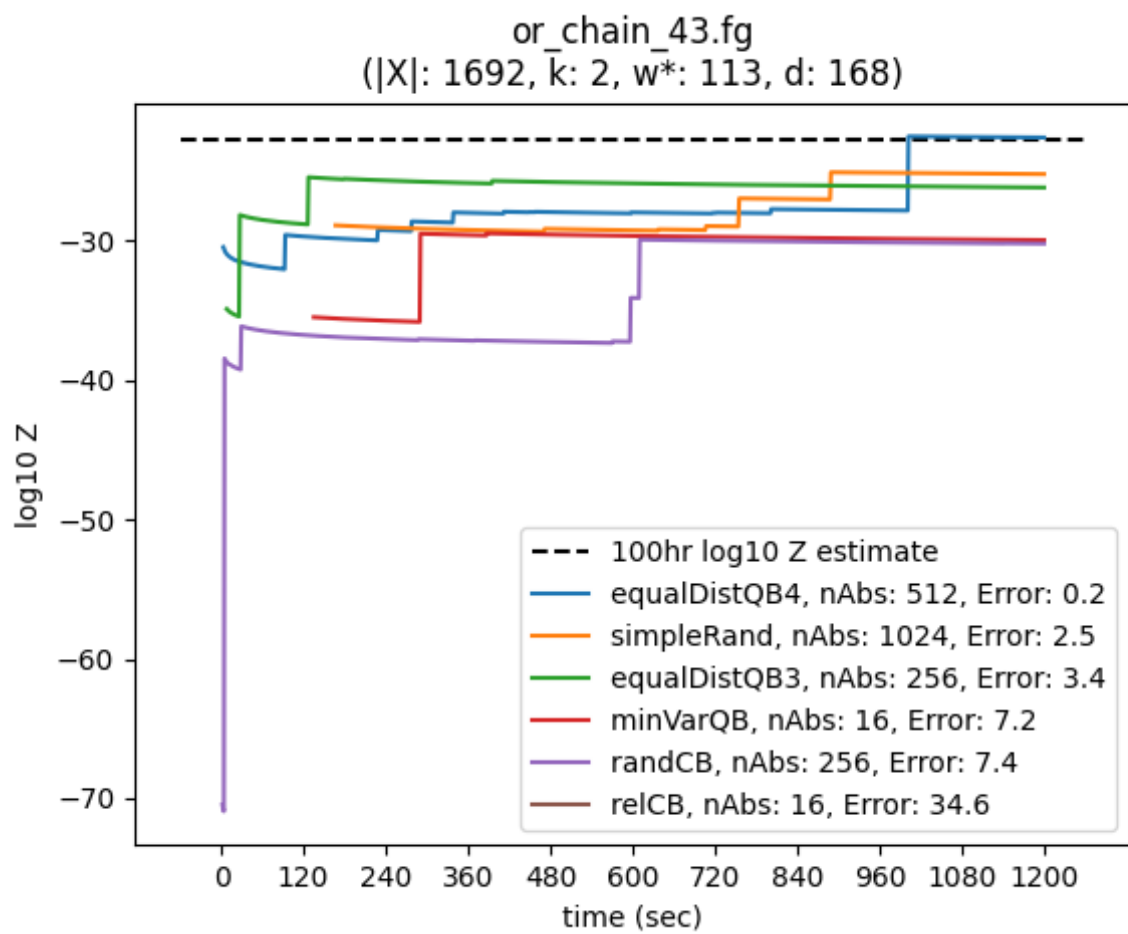
Plot 1: Z estimates from various algorithms versus time on DBN problem rus_100_200_7_1 using $iB = 10$. The dashed black line shows the estimated true Z value.



Plot 2: Z estimates from various algorithms versus time on Grids problem grid80x80.f10.wrap using $iB = 10$. The dashed black line shows the estimated true Z value.



Plot 3: Z estimates from various algorithms versus time on Linkage-Type4 problem grid20x20.f15 using $iB = 10$. The dashed black line shows the estimated true Z value.



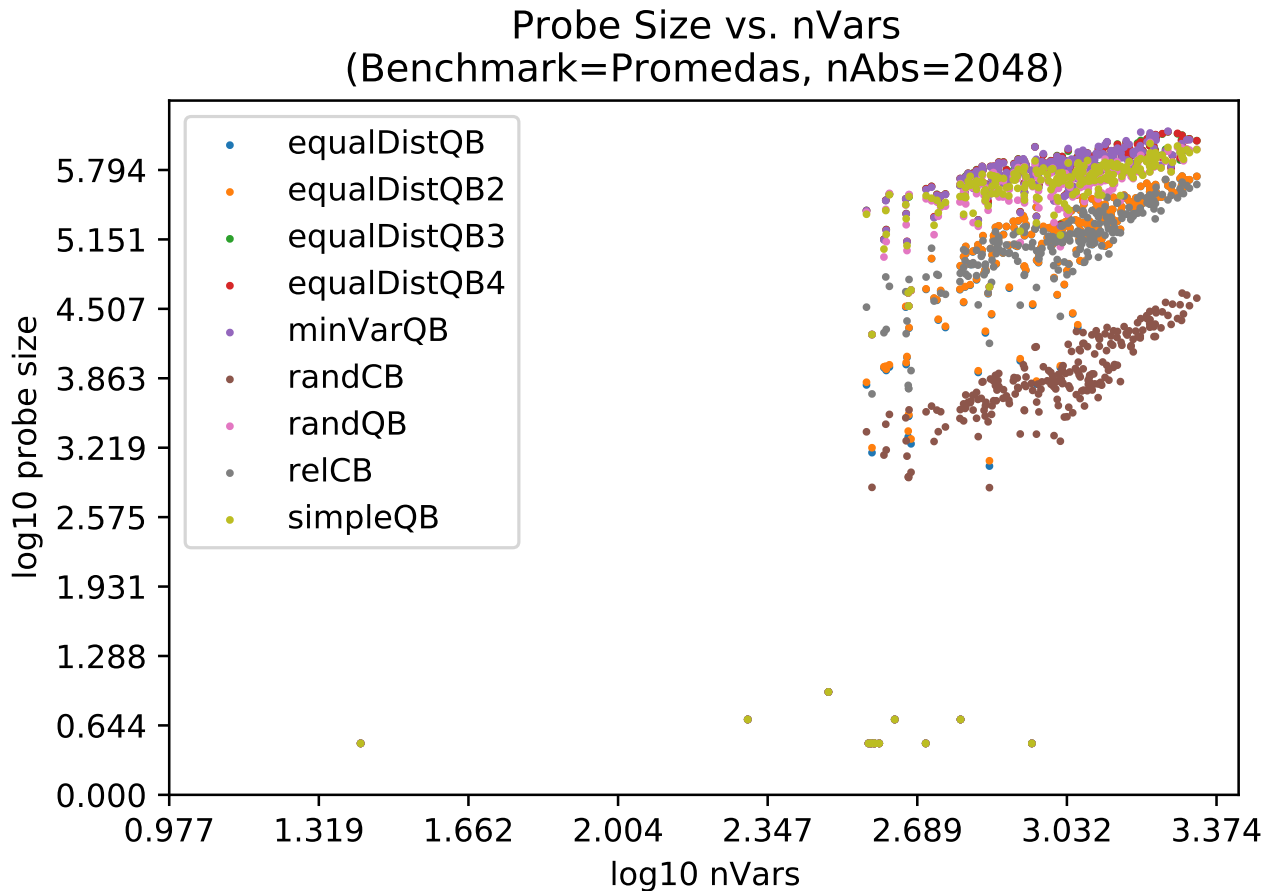
Plot 4: Z estimates from various algorithms versus time on Promedas problem or_chain_43.fg using $iB = 10$. The dashed black line shows the estimated true Z value.

8 ADDITIONAL RESULTS

8.1 PROBE SIZE

In our running abstraction example discussed in Supplemental Section 6, we observed that despite employing the same granularity, certain Ordered Partitioning Schemes may underutilize the allotted number of abstract states. Moreover, paths extended during initial iterations may become incomplete in subsequent iterations. These truncated paths may be pruned altogether and cut the number of nodes. To assess how effectively different schemes handle continual extension of paths, we fixed $n.Abs$ at 2048 and plotted the Probe Size against the number of variables for each problem in the Promedas benchmark (Plot 5).

Plot 5: For the given abstraction granularity and benchmark, the size of the probe (in log10) relative to the number of problem variables (in log10) using iB-10.



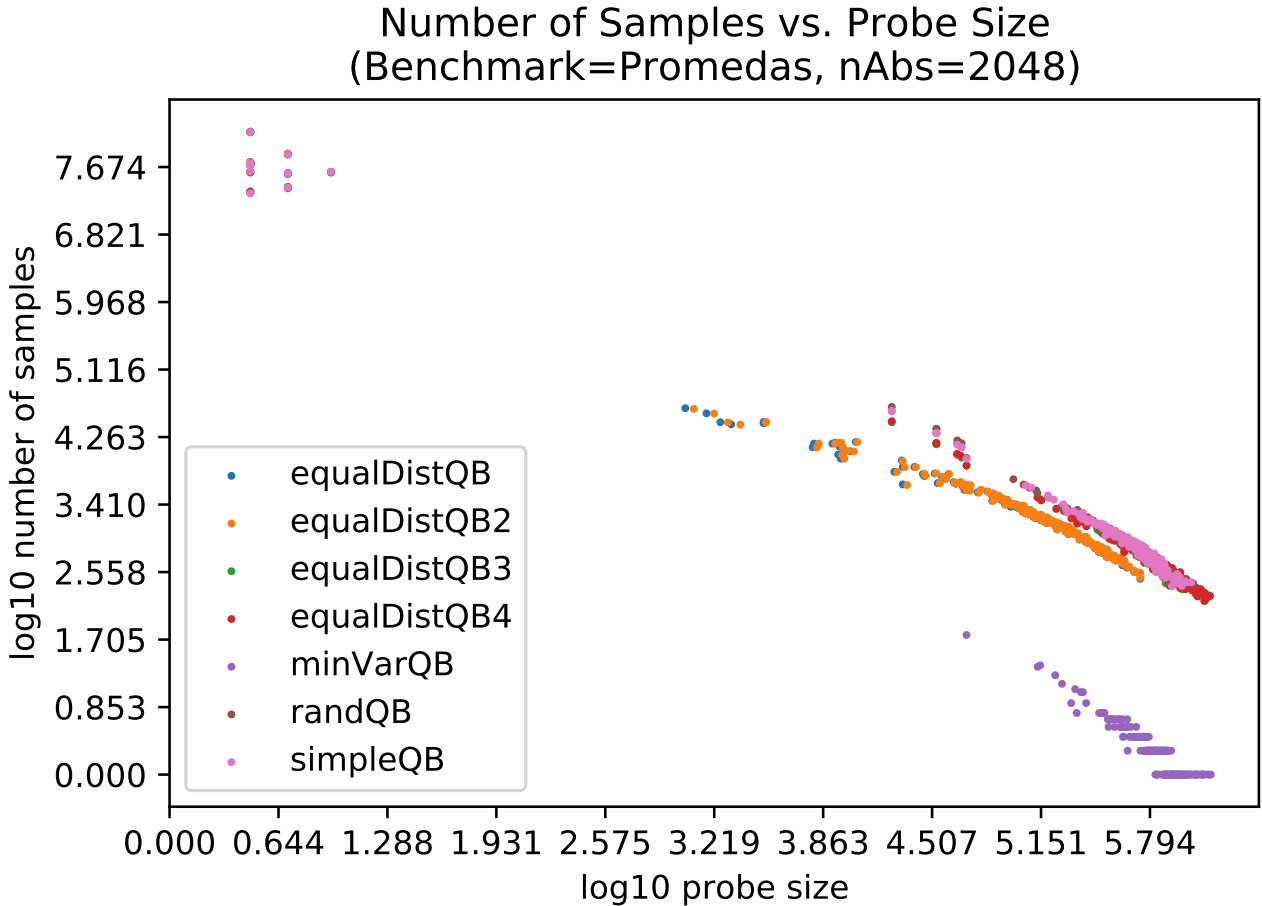
Even with the same granularity different abstraction functions can lead to vastly different utilization of abstract states, pruning, and thus probe sizes. Plot 5 highlights this. As seen in the plot (and generalizes across the different benchmarks and abstraction value classes) the simpleQB, minVarQB, equalDistQB3, equalDistQB4, and randQB schemes tend to produce larger probes, indicating more of the allotted abstract states utilized and fewer branches being pruned.

8.2 ABSTRACTION SPEED

In order to understand more about the speed of each scheme at performing abstractions, in Figure ?? we plot the number of samples versus average probe size for problems of the Promedas benchmark. (For other benchmarks and $n.Abs$, please see

the Supplemental Materials).

Plot 6: For the given abstraction granularity and benchmark, the number of samples (in log10) relative to the probe size (in log10) using iB-10.



Plot 6 shows the number of samples that were able to be drawn relative to the size of generated probes, thus providing an understanding of the speed abstractions occur. As expected, we notice the minVar scheme (which utilizes a computationally intensive hierarchical clustering process to abstract nodes) has the lowest sample efficiency. The other schemes have comparable abstraction speeds.

References

- Filjor Broka, Rina Dechter, Alexander Ihler, and Kalev Kask. Abstraction sampling in graphical models. In *Proceedings of the Thirty-Fourth Conference on Uncertainty in Artificial Intelligence, UAI 2018, Monterey, California, USA, August 6–10, 2018*, pages 632–641, 2018. URL <http://auai.org/uai2018/proceedings/papers/234.pdf>.
- H. Kahn and A. W. Marshall. Methods of reducing sample size in monte carlo computations. *Journal of the Operations Research Society of America*, 1(5):263–278, 1953. ISSN 00963984. URL <http://www.jstor.org/stable/166789>.
- Kalev Kask, Bobak Pezeshki, Filjor Broka, Alexander Ihler, and Rina Dechter. Scaling up and/or abstraction sampling. In Christian Bessiere, editor, *Proceedings of the Twenty-Ninth International Joint Conference on Artificial Intelligence, IJCAI-20*, pages 4266–4274. International Joint Conferences on Artificial Intelligence Organization, 7 2020. doi: 10.24963/ijcai.2020/589. URL <https://doi.org/10.24963/ijcai.2020/589>. Main track.
- G. N. Lance and W. T. Williams. A General Theory of Classificatory Sorting Strategies: 1. Hierarchical Systems. *The Computer Journal*, 9(4):373–380, 02 1967. ISSN 0010-4620. doi: 10.1093/comjnl/9.4.373. URL <https://doi.org/10.1093/comjnl/9.4.373>.
- Robert Mateescu, Rina Dechter, and Radu Marinescu. AND/OR multi-valued decision diagrams (aomdds) for graphical models. *J. Artif. Intell. Res. (JAIR)*, 33:465–519, 2008. doi: 10.1613/jair.2605. URL <http://dx.doi.org/10.1613/jair.2605>.
- Art B. Owen. *Monte Carlo theory, methods and examples*. <https://artowen.su.domains/mc/>, 2013.
- Maria L. Rizzo. *Statistical computing with R*. Chapman & Hall/CRC, 2007.
- Joe H. Ward. Hierarchical grouping to optimize an objective function. *Journal of the American Statistical Association*, 58(301):236–244, 1963. ISSN 01621459. URL <http://www.jstor.org/stable/2282967>.